

*Supporting Information*  
*for*

**Anticancer half-sandwich Ir(III) complex and its interaction  
with various biomolecules and their mixtures - a case study  
with ascorbic acid**

Lukáš Masaryk,<sup>a</sup> Jakub Orvoš,<sup>b</sup> Karolina Śloczyńska,<sup>c</sup> Radovan Herchel,<sup>a</sup> Ján Moncol,<sup>d</sup>  
David Milde,<sup>e</sup> Petr Halaš,<sup>a</sup> Radka Křikavová,<sup>a</sup> Karolina Śloczyńska,<sup>c</sup>  
Paulina Koczurkiewicz-Adamczyk,<sup>c</sup> Elżbieta Pękala,<sup>c</sup> Róbert Fischer,<sup>b</sup> Ivan Šalitroš,<sup>a,d</sup>  
Ivan Nemeč<sup>a</sup> and Pavel Štarha<sup>a,\*</sup>

<sup>a</sup> *Department of Inorganic Chemistry, Faculty of Science, Palacky University in Olomouc, 17.  
listopadu 12, 77146 Olomouc, Czech Republic*

<sup>b</sup> *Department of Organic Chemistry, Faculty of Chemical and Food Technology, Slovak  
University of Technology in Bratislava, Bratislava SK-81237, Slovakia*

<sup>c</sup> *Department of Pharmaceutical Biochemistry, Faculty of Pharmacy, Jagiellonian University  
Medical College, Medyczna 9, 30-688 Kraków, Poland*

<sup>d</sup> *Department of Inorganic Chemistry, Faculty of Chemical and Food Technology, Slovak  
University of Technology in Bratislava, Bratislava SK-81237, Slovakia*

<sup>e</sup> *Department of Analytical Chemistry, Faculty of Science, Palacký University in Olomouc, 17.  
listopadu 12, 771 46 Olomouc, Czech Republic*

\* E-mail (PŠ): [pavel.starha@upol.cz](mailto:pavel.starha@upol.cz)

## Table of Contents

Experimental section .....	S3
Table S1 - Crystallographic data for <b>1-3</b> .....	S12
Table S2 - Selected bond lengths and angles (X-ray analysis) .....	S13
Table S3 - Selected structural parameters (calculated by DFT) .....	S14
Scheme S1 - Synthesis of L <sup>1</sup> and L <sup>2</sup> .....	S15
Figure S1 - Structural formulas of selected anticancer benzimidazole derivatives. ....	S16
Figure S2, S3 - <sup>1</sup> H and <sup>13</sup> C NMR spectra of L <sup>1</sup> and L <sup>2</sup> .....	S17
Figure S4 - ESI+ mass spectra of complexes <b>1-3</b> .....	S19
Figure S5-S7 - <sup>1</sup> H and <sup>13</sup> C NMR spectrum of complex <b>1-3</b> .....	S20
Figure S8-S10 - Crystal structures and non-covalent interactions of <b>1-3</b> .....	S23
Figure S11-S13 - <sup>1</sup> H NMR stability studies for <b>1-3</b> .....	S26
Figure S14 - DFT investigation of hydrolysis of <b>1-3</b> .....	S29
Figure S15 - Fluorescence spectral studies of interaction with BSA .....	S30
Figure S16 - <sup>1</sup> H NMR studies of interaction with GMP .....	S31
Figure S17 - <sup>1</sup> H NMR studies of interaction of <b>3</b> with NADH .....	S32
Figure S18 - <sup>1</sup> H NMR studies of interaction of L <sup>2</sup> with NADH .....	S33
Figure S19 - UV/Vis spectral studies of interaction with NADH .....	S34
Figure S20 - Cyclic voltammograms of L <sup>1</sup> , L <sup>2</sup> and <b>1-3</b> .....	S35
Figure S21 - <sup>1</sup> H NMR studies of interaction with NADH .....	S36
Figure S22 - <sup>1</sup> H NMR characterization of the hydrazo form of <b>3</b> .....	S37
Figure S23 - Mass spectrometry of the hydrazo form of <b>3</b> .....	S38
Figure S24-S27 - <sup>1</sup> H NMR studies of interaction of <b>3</b> with GSH .....	S39
Figure S28 - <sup>1</sup> H NMR studies of interaction of L <sup>2</sup> with GSH .....	S43
Figure S29 - <sup>1</sup> H NMR studies of interaction of <b>1</b> and <b>2</b> with GSH .....	S44
Figure S30 - ESI+ mass spectra of the mixture of <b>3</b> with GSH .....	S45
Figure S31 - <sup>1</sup> H NMR studies of interaction of <b>3</b> with ASA .....	S46
Figure S32 - <sup>1</sup> H NMR studies of interaction of <b>3</b> with GSH and NADH .....	S47
Figure S33 - <sup>1</sup> H NMR studies of interaction of <b>3</b> with ASA and NADH .....	S48
Figure S34, S35 - <sup>1</sup> H NMR studies of interaction of <b>3</b> with GSH and ASA .....	S49
Figure S36 - ESI+ mass spectra of the mixture of <b>3</b> with GSH and ASA .....	S51
Figure S37 - <sup>1</sup> H NMR studies of interaction of <b>3</b> with GSH, NADH and ASA .....	S52
References .....	S53

## Experimental

### Materials

RuCl<sub>3</sub>·*n*H<sub>2</sub>O, IrCl<sub>3</sub>·*n*H<sub>2</sub>O, 4-methyl-1-(1-methylethyl)-1,3-cyclohexadiene ( $\alpha$ -terpinene), 1,2,3,4,5-pentamethylcyclopenta-1,3-diene (HCp\*), 5-aminopicolinic acid, 6-aminopicolinic acid, *o*-phenylenediamine, *N,N*-diisopropylethylamine (DIPEA), *O*-(benzotriazol-1-yl)-*N,N,N',N'*-tetramethyluronium tetrafluoroborate (TBTU), nitrosobenzene, tetrabutylammonium bromide (TBAB), sodium hydroxide (NaOH), sodium hydrogen carbonate (NaHCO<sub>3</sub>), magnesium sulfate (MgSO<sub>4</sub>), ammonium hexafluorophosphate (NH<sub>4</sub>PF<sub>6</sub>), bovine serum albumin (BSA),  $\beta$ -nicotinamide adenine dinucleotide reduced, disodium salt (NADH),  $\beta$ -nicotinamide adenine dinucleotide, hydrate (NAD<sup>+</sup>), guanosine 5'-monophosphate disodium salt hydrate (GMP), L-ascorbic acid (ASA), L-dehydroascorbic acid (DHA), phosphate-buffered saline (PBS), tris(hydroxymethyl)aminomethane (tris) buffer, potassium chloride (KCl), sodium chloride (NaCl), solvents (methanol (MeOH), diethyl ether, ethanol, *N,N*-dimethylformamide (DMF), dimethyl sulfoxide (DMSO), acetic acid (AcOH), pyridine, ethyl acetate (EtOAc), dichloromethane (DCM), hexanes, *n*-heptane, *n*-butyl acetate, acetone, toluene, ammonia aqueous 25–27% (NH<sub>3</sub>), acetonitrile (CH<sub>3</sub>CN) and *n*-octanol) and deuterated solvents for NMR experiments (DMSO-*d*<sub>6</sub>, D<sub>2</sub>O) were supplied by VWR International (Střbrná Skalice, Czech Republic), Sigma-Aldrich (Prague, Czech Republic), Lach-Ner (Neratovice, Czech Republic), Litolab (Chudobín, Czech Republic), Fluorochem (Hadfield, UK), TCI EUROPE N.V. (Zwijndrecht, Belgium), Alfa Aesar (Kandel, Germany) and Mikrochem Trade (Pezinok, Slovak Republic). The used chemicals and solvents were used as received.

The starting dimeric complexes, [Ru( $\mu$ -Cl)( $\eta^6$ -pcym)Cl]<sub>2</sub> and [Ir( $\mu$ -Cl)( $\eta^5$ -Cp\*)Cl]<sub>2</sub>,<sup>1,2</sup> were synthesized in a Monowave 300 microwave reaction system (Anton Paar), as described previously.<sup>3,4</sup>

### Synthesis of organic derivatives L<sup>1</sup>–L<sup>2</sup>

**5-Amino-*N*-(2-aminophenyl)pyridine-2-carboxamide (I).** To a stirred solution of 5-aminopicolinic acid (1.00 g, 7.24 mmol) in anhydrous DMF (120 mL) at room temperature (r.t.) DIPEA (2.52 mL, 14.48 mmol) and *o*-phenylenediamine (1.17 g, 10.86 mmol) were sequentially added. The resulting mixture was cooled down to 0 °C, and TBTU (2.56 g, 7.96 mmol) was added. After stirring for 10 min, the cooling bath was removed, and stirring was continued at r.t. for 22 h. After this time, the reaction mixture was concentrated under reduced pressure, the residue was dissolved in DCM (100 mL), and the solution was sequentially washed with sat. aq. NaHCO<sub>3</sub> (100 mL) and aqueous acetic acid (100 mL, 0.5% v/v). The organic layer was dried over MgSO<sub>4</sub>, and the solvent was evaporated under reduced pressure. The residue was purified by flash column chromatography (FCC; DCM/MeOH, 97:3) to give amide I (0.95 g, 4.16 mmol, 57 %) as a yellowish solid; R<sub>f</sub> = 0.26 (DCM/MeOH, 98:2); m.p. 168–170 °C. <sup>1</sup>H NMR (300 MHz, DMSO-*d*<sub>6</sub>, 298 K, ppm):  $\delta$  9.70 (bs, 1H, CO–NH), 8.00 (d,

$J = 2.7$  Hz, 1H, C6-H), 7.83 (d,  $J = 8.6$  Hz, 1H, C3-H), 7.54 (dd,  $J = 1.4, 7.9$  Hz, 1H, Ph-H), 7.03 (dd,  $J = 2.7, 8.6$  Hz, 1H, C4-H), 6.94–6.88 (m, 1H, Ph-H), 6.82 (dd,  $J = 1.5, 7.9$  Hz, 1H, Ph-H), 6.67–6.61 (m, 1H, Ph-H), 6.05 (bs, 2H, C5-NH<sub>2</sub>), 4.81 (bs, 2H, Ph-NH<sub>2</sub>). <sup>13</sup>C NMR (75 MHz, DMSO-*d*<sub>6</sub>, 298 K, ppm):  $\delta$  162.7, 147.7, 141.1, 137.3, 134.3, 125.1, 125.0, 123.7, 123.3, 119.3, 117.2, 116.9. HRMS (ESI+,  $m/z$ ): 229.1083 (calc. 229.1084 for [M+H]<sup>+</sup> (C<sub>12</sub>H<sub>13</sub>N<sub>4</sub>O)). IR (ATR,  $\nu$ , cm<sup>-1</sup>): 748, 857, 1013, 1130, 1234, 1471, 1510, 1574, 1614, 1652, 3192, 3303, 3404, 3438.

**6-Amino-*N*-(2-aminophenyl)pyridine-2-carboxamide (II).** Compound **II** was prepared by analogical synthesis as described above for **I**, but the synthesis of **II** started from 6-aminopicolinic acid (instead of 5-aminopicolinic acid used for **I**) with 25 h reaction time (instead of 22 h used for **I**). The residue was purified by FCC (DCM/EtOAc, 1:1) to give amide **II** (0.90 g, 3.94 mmol, 54 %) as a yellowish solid;  $R_f = 0.24$  (DCM/EtOAc, 1:1); m.p. 139–141 °C. <sup>1</sup>H NMR (300 MHz, DMSO-*d*<sub>6</sub>, 298 K, ppm):  $\delta$  9.74 (bs, 1H, CO-NH), 7.59 (dd,  $J = 7.2, 8.3$  Hz, 1H, C4-H), 7.60–7.55 (m, 1H, Ph-H), 7.27 (dd,  $J = 0.9, 7.3$  Hz, 1H, C3-H), 6.94 (ddd,  $J = 1.5, 7.2, 7.9$  Hz, 1H, Ph-H), 6.83 (dd,  $J = 1.5, 8.0$  Hz, 1H, Ph-H), 6.69 (dd,  $J = 0.9, 8.3$  Hz, 1H, C5-H), 6.65 (ddd,  $J = 1.5, 7.2, 7.9$  Hz, 1H, Ph-H), 6.26 (bs, 2H, C6-NH<sub>2</sub>), 4.87 (bs, 2H, Ph-NH<sub>2</sub>). <sup>13</sup>C NMR (75 MHz, DMSO-*d*<sub>6</sub>, 298 K, ppm):  $\delta$  162.5, 158.5, 147.9, 141.0, 138.3, 125.5, 124.1, 123.4, 117.1, 116.7, 111.6, 110.1. HRMS (ESI+,  $m/z$ ): 229.1082 (calc. 229.1084 for [M+H]<sup>+</sup> (C<sub>12</sub>H<sub>13</sub>N<sub>4</sub>O)). IR (ATR,  $\nu$ , cm<sup>-1</sup>): 740, 815, 988, 1274, 1358, 1431, 1452, 1519, 1590, 1633, 1669, 3167, 3308, 3353, 3373.

**6-(1*H*-Benzimidazol-2-yl)pyridin-3-amine (III).** Amide **I** (0.94 g, 4.12 mmol) was dissolved in acetic acid (20 mL), and the resulting solution was heated at 100 °C for 1 h. After this time, the solvent was evaporated *in vacuo*, and the residue was co-evaporated with *n*-heptane (2 × 20 mL). The product was purified by FCC (DCM/MeOH/NH<sub>3</sub>, 14:1:0.1) to give benzimidazole derivative **III** (0.81 g, 3.83 mmol, 93 %) as a yellowish foam;  $R_f = 0.20$  (DCM/MeOH/NH<sub>3</sub>, 14:1:0.1); m.p. 210–216 °C. <sup>1</sup>H NMR (600 MHz, DMSO-*d*<sub>6</sub>, 298 K, ppm):  $\delta$  12.61 (bs, 1H, N1-H), 8.05 (d,  $J = 2.7$  Hz, 1H, C10-H), 7.99 (d,  $J = 8.5$  Hz, 1H, C13-H), 7.60–7.42 (m, 2H, C4-H, C7-H), 7.16–7.09 (m, 2H, C5-H, C6-H), 7.06 (dd,  $J = 2.7, 8.5$  Hz, 1H, C12-H), 5.84 (bs, 2H, C11-NH<sub>2</sub>). <sup>13</sup>C NMR (150 MHz, DMSO-*d*<sub>6</sub>, 298 K, ppm):  $\delta$  152.0, 146.1, 136.2, 143.7, 135.3, 135.2, 122.3, 121.5 (× 2), 120.1, 117.8, 111.9. HRMS (ESI+,  $m/z$ ): 211.0979 (calc. 211.0979 for [M+H]<sup>+</sup> (C<sub>12</sub>H<sub>11</sub>N<sub>4</sub>)). IR (ATR,  $\nu$ , cm<sup>-1</sup>): 545, 739, 829, 968, 1272, 1402, 1421, 1588, 1648, 3191, 3325, 3424.

**6-(1*H*-Benzimidazol-2-yl)pyridin-2-amine (IV).** This compound was prepared as described for **III**, with amide **II** (0.82 g, 3.59 mmol) used as the key intermediate. The product was purified by FCC (DCM/MeOH/NH<sub>3</sub>, 19:1:0.1) to give benzimidazole derivative **IV** (0.71 g, 3.38 mmol, 94 %) as a yellowish solid;  $R_f = 0.28$  (DCM/MeOH/NH<sub>3</sub>, 50:1:0.1); m.p. 231–233 °C, decomposition. <sup>1</sup>H NMR (600 MHz, DMSO-*d*<sub>6</sub>, 298 K, ppm):  $\delta$  12.56 (bs, 1H, N1-H), 7.64–7.54 (m, 2H, C4-H, C7-H), 7.56 (dd,  $J = 7.5, 8.1$  Hz, 1H, C12-H), 7.48 (dd,  $J = 0.7, 7.3$  Hz, 1H, C13-H), 7.20–7.17 (m, 2H, C5-H, C6-H), 6.60 (dd,  $J = 0.6, 8.1$  Hz, 1H, C11-H), 5.99 (bs, 2H, C10-NH<sub>2</sub>). <sup>13</sup>C NMR (75 MHz, DMSO-*d*<sub>6</sub>, 298 K, ppm):  $\delta$  159.4, 151.4, 146.6, 143.9, 138.0, 134.7, 122.5, 121.6, 119.0, 112.0, 110.0, 109.3. HRMS (ESI+,  $m/z$ ): 211.0980 (calc. 211.0979

for  $[M+H]^+$  ( $C_{12}H_{11}N_4$ ). IR (ATR,  $\nu$ ,  $cm^{-1}$ ): 742, 803, 985, 1276, 1308, 1402, 1468, 1570, 1609, 3306, 3469.

**2-{5-[(E)-phenyldiazenyl]pyridin-2-yl}-1H-benzimidazole (L<sup>1</sup>).** To a well-stirred solution of **III** (0.80 g, 3.81 mmol) in pyridine (18 mL) at 50 °C, TBAB (0.25 g, 0.76 mmol) and aqueous NaOH solution (2.03 mL, 38.1 mmol, 50% w/w) were sequentially added. After 10 min of stirring, nitrosobenzene (0.82 g, 7.62 mmol) was added and the resulting mixture was stirred at 50 °C for 3 h. After this time, a second portion of nitrosobenzene (0.41 g, 3.82 mmol) was added, and stirring was continued at the same temperature for additional 2 h. Then, the reaction mixture was cooled down to r.t., diluted with DCM (100 mL) and washed with water (2 × 100 mL) and brine (100 mL). The organic layer was dried over  $MgSO_4$ , and the solvent was evaporated *in vacuo*. After co-evaporation with toluene (2 × 20 mL), the solid residue was triturated with hexanes (2 × 30 mL) and crystallized from *n*-butyl acetate to give the final product L<sup>1</sup> (0.98 g, 3.27 mmol, 86 %) as an orange crystalline powder;  $R_f$  = 0.38 (DCM/ $CH_3CN/NH_3$ , 32:1:0.1); m.p. 239–253 °C. <sup>1</sup>H NMR (300 MHz,  $DMSO-d_6$ , 298 K, ppm):  $\delta$  13.32 (bs, 1H, N1-H), 9.28 (dd,  $J$  = 0.6, 2.3 Hz, 1H, C10-H), 8.54 (dd,  $J$  = 0.6, 8.5 Hz, 1H, C13-H), 8.37 (dd,  $J$  = 2.3, 8.5 Hz, 1H, C12-H), 8.01–7.95 (m, 2H, C15-H), 7.76–7.57 (m, 5H, C4-H, C7-H, C16-H, C17-H), 7.32–7.22 (m, 2H, C5-H, C6-H). <sup>13</sup>C NMR (75 MHz,  $DMSO-d_6$ , 298 K, ppm):  $\delta$  152.0, 150.4, 149.8, 147.4, 146.9, 144.0, 135.2, 132.3, 129.6, 127.8, 123.7, 122.9, 122.3, 122.2, 119.5, 112.2. HRMS (ESI+,  $m/z$ ): 300.1243 (calc. 300.1244 for  $[M+H]^+$  ( $C_{18}H_{14}N_5$ )). IR (ATR,  $\nu$ ,  $cm^{-1}$ ): 444, 550, 681, 737, 854, 1109, 1147, 1267, 1316, 1422, 1437, 1591, 3055.

**2-{6-[(E)-phenyldiazenyl]pyridin-2-yl}-1H-benzimidazole (L<sup>2</sup>).** Compound **IV** (0.7 g, 3.33 mmol) was stirred at 50 °C in pyridine (17 mL) with sequentially added TBAB (0.22 g, 0.67 mmol) and aqueous NaOH solution (1.78 mL; 33.3 mmol, 50% w/w) for 10 min. After that, nitrosobenzene (0.71 g, 6.66 mmol) was added and the mixture was stirred for the next 90 min (50 °C). Then, the second portion of nitrosobenzene (0.36 g; 3.33 mmol) was added. The reaction mixture was cooled down to r.t. after the additional 2 h of stirring at 50 °C, diluted with DCM (100 mL) and washed with water (2 × 100 mL) and brine (100 mL). The separated organic layer was dried with  $MgSO_4$ , and the dried solution was evaporated *in vacuo*. After co-evaporation with toluene (2 × 20 mL), the solid residue was triturated with hexanes (2 × 30 mL) and purified by FCC (DCM/acetone, 92:8) to give L<sup>2</sup> (0.84 g, 2.81 mmol, 83 %) as a brick-coloured powder;  $R_f$  = 0.19 (DCM/acetone, 94:6); m.p. 187–189 °C. <sup>1</sup>H NMR (600 MHz,  $DMSO-d_6$ , 298 K, ppm):  $\delta$  13.23 (bs, 1H, N1-H), 8.51 (dd,  $J$  = 0.8, 7.7 Hz, 1H, C13-H), 8.23 (pseudo t,  $J$  = 7.8, 7.9 Hz, 1H, C12-H), 8.03–7.99 (m, 2H, C15-H), 7.78 (dd,  $J$  = 0.8, 7.9 Hz, 1H, C11-H), 7.76–7.59 (m, 5H, C4-H, C7-H, C16-H, C17-H), 7.29–7.23 (m, 2H, C5-H, C6-H). <sup>13</sup>C NMR (150 MHz,  $DMSO-d_6$ , 298 K, ppm):  $\delta$  162.8, 151.8, 149.9, 148.5, 143.8, 140.3, 135.1, 132.8, 129.7, 123.4, 123.2, 123.1, 122.1, 119.4, 112.9, 112.4. HRMS (ESI+,  $m/z$ ): 300.1254 (calc. 300.1244 for  $[M+H]^+$  ( $C_{18}H_{14}N_5$ )). IR (ATR,  $\nu$ ,  $cm^{-1}$ ): 526, 687, 738, 813, 991, 1151, 1275, 1313, 1387, 1414, 1565, 1591, 3053.

## Synthesis of complexes

Complexes **1–3** were prepared by the reaction of 0.05 mmol of either [Ru( $\mu$ -Cl)( $\eta^6$ -pcym)Cl]<sub>2</sub> (for **1**) or [Ir( $\mu$ -Cl)( $\eta^5$ -Cp\*)Cl]<sub>2</sub> (for **2** and **3**), with 0.10 mmol of 2-(pyridin-2-yl)-1*H*-benzimidazole-based ligands L<sup>1</sup> (for **1** and **2**) or L<sup>2</sup> (for **3**), stirred in MeOH (5 mL) at r.t. for 24 h. Within this period of time, the starting suspensions changed to solutions containing complexes [Ru( $\eta^6$ -pcym)Cl(L<sup>1</sup>)]Cl (**1\***), [Ir( $\eta^5$ -Cp\*)Cl(L<sup>1</sup>)]Cl (**2\***) or [Ir( $\eta^5$ -Cp\*)Cl(L<sup>2</sup>)]Cl (**3\***). Then, an excess of NH<sub>4</sub>PF<sub>6</sub> (0.25 mmol) was added and after 5 min of stirring at r.t. the reaction mixture was filtered and the solvent volume was reduced by the nitrogen gas until an orange product precipitated. Complexes **1–3** were collected, washed (1 × 0.5 mL of MeOH and 3 × 1.0 mL of diethyl ether) and dried in a desiccator under reduced pressure.

**[Ru( $\eta^6$ -pcym)Cl(L<sup>1</sup>)]PF<sub>6</sub> (**1**):** Red solid. Yield: 85 %. C<sub>28</sub>H<sub>27</sub>N<sub>5</sub>ClF<sub>6</sub>PRuH<sub>2</sub>O (MW = 715.0). Anal. calc.: C, 45.88, H, 3.99, N, 9.55; found: C, 45.50, H, 3.72, N, 9.32 %. <sup>1</sup>H NMR (400 MHz, DMSO-*d*<sub>6</sub>, 298 K, ppm):  $\delta$  10.09 (s, 1H, C10-H), 8.69–8.54 (m, 2H, C12-H, C13-H), 8.18–8.11 (m, 1H, C4-H), 8.08–8.02 (m, 2H, C15-H), 7.89–7.80 (m, 1H, C7-H), 7.75–7.66 (m, 3H, C16-H, C17-H), 7.63–7.54 (m, 2H, C5-H, C6-H), 6.48 (d, *J* = 6.6 Hz, 2H, C19-H), 6.24 (d, *J* = 6.6 Hz, 2H, C20-H), 2.57–2.48 (m, 1H, C21-H), 2.21 (s, 3H, C24-H), 0.91–0.86 (m, 6H, C23-H). <sup>13</sup>C NMR (101 MHz, DMSO-*d*<sub>6</sub>, 298 K, ppm):  $\delta$  154.7, 152.4, 149.8, 148.9, 147.6, 141.7, 134.8, 133.9, 130.3, 130.1, 127.0, 125.7, 124.2, 123.8, 118.8, 114.5, 105.9, 103.5, 86.3, 84.4, 82.7, 79.9, 31.0, 22.4, 22.1, 19.2. MS (ESI+, *m/z*): 570.2 (calc. 570.1 for [RuCl(L<sup>1</sup>)(pcym)]<sup>+</sup> (100 %), 534.3 (calc. 534.1 for {[Ru(L<sup>1</sup>)(pcym)]-H}<sup>+</sup> (29 %). IR (ATR,  $\nu$ , cm<sup>-1</sup>): 399, 456, 467, 556, 652, 688, 697, 746, 767, 832s, 939, 1033, 1102, 1151, 1266, 1298, 1361, 1388, 1456, 1454, 1491, 1632, 2241, 2286, 2331, 3221.

**[Ir( $\eta^5$ -Cp\*)Cl(L<sup>1</sup>)]PF<sub>6</sub> (**2**):** Orange solid. Yield: 92 %. C<sub>28</sub>H<sub>29</sub>N<sub>5</sub>ClF<sub>6</sub>IrP (MW = 808.2). Anal. calc.: C, 41.61, H, 3.62, N, 8.67; found: C, 41.29, H, 3.40, N, 8.32 %. <sup>1</sup>H NMR (400 MHz, DMSO-*d*<sub>6</sub>, 298 K, ppm):  $\delta$  9.43 (s, 1H, C10-H), 8.80 (d, *J* = 8.5 Hz, 1H, C12-H), 8.71 (d, *J* = 8.5 Hz, 1H, C13-H), 8.07–8.03 (m, 2H, C15-H), 7.88 (d, *J* = 7.9 Hz, 1H, C7-H), 7.79 (d, *J* = 7.9 Hz, 1H, C4-H), 7.69 (s, 3H, C16-H, C17-H), 7.63–7.54 (m, 2H, C5-H, C6-H), 1.75 (s, 15H, C19-H). <sup>13</sup>C NMR (101 MHz, DMSO-*d*<sub>6</sub>, 298 K, ppm):  $\delta$  152.3, 152.3, 149.5, 148.4, 147.8, 139.1, 135.2, 134.0, 132.8, 130.3, 126.9, 125.9, 124.5, 124.0, 117.4, 115.0, 89.2, 9.5. MS (ESI+, *m/z*): 662.3 (calc. 662.2 for [IrCl(Cp\*)(L<sup>1</sup>)]<sup>+</sup> (100 %), 626.4 (calc. 626.2 for {[Ir(Cp\*)(L<sup>1</sup>)]-H}<sup>+</sup> (23 %). IR (ATR,  $\nu$ , cm<sup>-1</sup>): 393, 462, 555, 631, 688, 746, 777, 831, 934, 1032, 1147, 1270, 1298, 1328, 1378, 1462, 1490, 1613, 2220, 2265, 2310, 3120.

**[Ir( $\eta^5$ -Cp\*)Cl(L<sup>2</sup>)]PF<sub>6</sub> (**3**):** Red solid. Yield: 89 %. C<sub>28</sub>H<sub>29</sub>N<sub>5</sub>ClF<sub>6</sub>IrP (MW = 808.2). Anal. calc.: C, 41.61, H, 3.62, N, 8.67; found: C, 41.35, H, 3.31, N, 8.40 %. <sup>1</sup>H NMR (400 MHz, DMSO-*d*<sub>6</sub>, 298 K, ppm):  $\delta$  8.62 (d, *J* = 7.8 Hz, 1H, C13-H), 8.55 (t, *J* = 7.8 Hz, 1H, C12-H), 8.08 (d, *J* = 7.8, 1H, C11-H), 8.03–7.97 (m, 2H, C15-H), 7.88 (d, *J* = 7.9 Hz, 1H, C7-H), 7.76–7.69 (m, 4H, C4-H, C16-H, C17-H), 7.61–7.52 (m, 2H, C5-H, C6-H), 1.43 (s, 15H, C19-H). <sup>13</sup>C NMR (101 MHz, DMSO-*d*<sub>6</sub>, 298 K, ppm):  $\delta$  162.2, 158.7, 152.4, 152.1, 147.4, 144.0, 138.5, 134.6, 130.3, 126.6, 125.6, 124.7, 124.2, 117.6, 115.8, 115.1, 88.9, 9.5. MS (ESI+, *m/z*): 662.3 (calc. 662.2 for [IrCl(Cp\*)(L<sup>2</sup>)]<sup>+</sup> (100 %), 626.4 (calc. 626.2 for {[Ir(Cp\*)(L<sup>2</sup>)]-H}<sup>+</sup> (37 %). IR (ATR,  $\nu$ , cm<sup>-1</sup>):

<sup>1</sup>): 437, 556, 638, 688, 707, 750, 832, 1008, 1028, 1074, 1149, 1196, 1231, 1296, 1325, 1381, 1415, 1442, 1481, 1569, 1609, 2212, 2252, 2294, 3432.

## General Methods

Electrospray ionization mass spectrometry (ESI-MS; methanol solutions) was carried out with an LCQ Fleet ion trap spectrometer (Thermo Scientific; QualBrowser software, version 2.0.7) in the positive ionization mode (ESI+). HRMS analysis was carried out with an Orbitrap Velos Pro spectrometer (Thermo Fisher Scientific).

<sup>1</sup>H and <sup>13</sup>C NMR spectroscopy, and <sup>1</sup>H-<sup>13</sup>C gs-HMQC and <sup>1</sup>H-<sup>13</sup>C gs-HMBC correlation experiments were recorded using DMSO-*d*<sub>6</sub> solutions at 298 K on a Varian-400 spectrometer (<sup>1</sup>H, 400.00 MHz, and <sup>13</sup>C, 101.00 MHz), on a Varian INOVA-300 spectrometer (<sup>1</sup>H, 299.95 MHz, and <sup>13</sup>C, 75.42 MHz) and on a Varian VNMRS-600 instrument (<sup>1</sup>H, 599.75 MHz, and <sup>13</sup>C, 150.81 MHz); gs = gradient selected, HMQC = heteronuclear multiple quantum coherence, HMBC = heteronuclear multiple bond coherence. <sup>1</sup>H and <sup>13</sup>C NMR spectra were calibrated against the residual DMSO signals: <sup>1</sup>H at 2.47 ppm and <sup>13</sup>C at 39.9 ppm. The splitting of proton resonances in the reported <sup>1</sup>H spectra is defined as s = singlet, d = doublet, dd = doublet of doublets, ddd = doublet of doublet of doublets, t = triplet, m = multiplet and bs = broad signal.

A Jasco FT/IR-4700 spectrometer (Jasco, Easton, MD, USA) was used for the collection of the Fourier-transform infrared (FTIR) spectra of the studied ligands and complexes in the range of 400–4000 cm<sup>-1</sup> by using the attenuated total reflection (ATR) technique on a diamond plate. Elemental analysis was performed by a Flash 2000 CHNS Elemental Analyser (Thermo Scientific; Waltham, MA, USA). For cyclic voltammetry potentiostat CHI600C (CH Instruments) was used.

Melting points were measured with a Melting Point B-540 apparatus (Büchi). Flash column chromatography (FCC) was carried out with a Büchi system (Pump Manager C-615 and Fraction Collector C-660) using Normasil 60 silica gel (0.040–0.063 mm; VWR). Thin Layer Chromatography (TLC) analysis was carried out using TLC silica gel 60 F254 (aluminium sheets, Merck), and plates were visualized with UV light or by treatment with permanganate solution followed by heating.

The determination of the Ru and Ir content was performed using ICP-MS (Agilent 7700x, Agilent Japan) in a He mode to overcome potential interferences. External calibration was applied, and internal standard correction used. Calibration solutions were prepared by diluting a multi elemental certified reference material – water calibration solution (obtained from Analytika Ltd., Czech Republic) with concentration 100.0±0.2 mg/L of each metal. All samples were diluted accordingly with deionized water prior to ICP-MS analysis.

## Crystallography

Data collection and cell refinement of **1**, **2**·2MeOH·H<sub>2</sub>O and **3** were carried out using a Stoe StadiVari diffractometer. The diffractometer is equipped by a Pilatus3R 300K HPAD

detector and microfocused X-ray source Xenocs Genix3D Cu HF (CuK $\alpha$  radiation,  $\lambda = 1.54186$  Å). The diffraction intensities of all three compounds were corrected for Lorentz and polarization factors. The multi-scan absorption corrections were applied using the program Stoe LANA software.<sup>5</sup> The structures were solved using SuperFlip<sup>6</sup> or ShelXT<sup>7</sup> programs and refined by the full-matrix least-squares procedure with ShelXL (version 2018/3)<sup>8</sup> or Olex2.refine (version 1.3).<sup>9</sup> Geometrical analyses were performed with ShelXL/Olex2.refine. The structures were drawn with OLEX2.<sup>10</sup> The unknown solvent molecules in the crystal structure of **3** were masked using solvent-masking utility in OLEX2 package. Crystallographic data for **1–3** are given below in Table S1.

### Studies of solvolysis

The appropriate amounts of complexes **1–3** for the preparation of 0.5 mM solutions were dissolved in (a) 250  $\mu$ L of DMSO- $d_6$  and 250  $\mu$ L of PBS in D<sub>2</sub>O (pH 7.4) or 250  $\mu$ L of DMF- $d_7$  and 250  $\mu$ L of PBS in D<sub>2</sub>O (pH 7.4). The prepared solutions were measured using <sup>1</sup>H NMR spectroscopy at various time points (0 h, 1 h and 24 h) and incubated at ambient temperature between the individual <sup>1</sup>H NMR experiments. For comparative purposes, 0.5 mM **3** was also studied in the mixture of 250  $\mu$ L of DMF- $d_7$  and 250  $\mu$ L of D<sub>2</sub>O either without or with a stoichiometric amount of AgNO<sub>3</sub>. The obtained <sup>1</sup>H NMR spectra were referenced to the residual signal of DMSO- $d_6$  (2.50 ppm) or DMF- $d_7$  (8.03 ppm). *Note:* DMSO- $d_6$  and DMF- $d_7$  ensured the solubility of all the tested complexes, as their solubility in water is very low.

### Studies of lipophilicity (log *P*)

Octanol-saturated water (OSW) and water-saturated octanol (WSO) were prepared from *n*-octanol and 0.2 M water solution of KCl (to suppress the hydrolysis) by overnight stirring. The stock solutions were prepared by shaking of 1 mmol of complexes **1–3** in 11 mL of OSW for 1 h. Then the mixtures were centrifuged (5 min, 11,000 rpm) and the supernatant was collected. 5 mL of this solution was studied by ICP-MS (to assess [M]<sub>OSWb</sub> as the metal concentration before partition), while other 5 mL of this solution was added to 5 mL of WSO and shaken for 2 h at r.t. After that, these mixtures were centrifuged, and aqueous layers were carefully separated. The Ru and Ir concentrations were determined by ICP-MS (the obtained values were corrected for the adsorption effects). The equation  $\log P = \log([M]_{\text{WSO}}/[M]_{\text{OSWa}})$  was used for the partition coefficient calculation, where [M]<sub>OSWa</sub> stands for the metal concentration after partition, and  $[M]_{\text{WSO}} = [M]_{\text{OSWb}} - [M]_{\text{OSWa}}$ . The experiment was conducted in triplicate and the results are presented as arithmetic mean $\pm$ SD.

### Interaction with biomolecules

5 molar equiv. of GSH, GMP, BSA, ASA or NADH were added to the solutions of the selected complexes (0.5 mM) in 250  $\mu$ L of DMSO- $d_6$  and 250  $\mu$ L of PBS in D<sub>2</sub>O (pH 7.4) (for GMP, BSA, GSH or NADH) or 250  $\mu$ L of DMF- $d_7$  and 250  $\mu$ L of PBS in D<sub>2</sub>O (pH 7.4) (for GSH, NADH, GSH/NADH (**A**), NADH/ASA (**B**), GSH/ASA (**C**) and GSH/NADH/ASA (**D**)). The

prepared solutions were measured using  $^1\text{H}$  NMR spectroscopy at various time points (0–24 h) and incubated at ambient temperature between the individual  $^1\text{H}$  NMR experiments. The obtained spectra were referenced to the residual signal of  $\text{DMSO-}d_6$  (2.50 ppm) or  $\text{DMF-}d_7$  (8.03 ppm). The control experiments were carried out in the same mixture of solvents with free biomolecules (GSH, ASA, NADH) and their mixtures (GSH/NADH, NADH/ASA, GSH/ASA and GSH/NADH/ASA) and for  $L^2$  in the presence of excess of GSH, ASA, NADH, GSH/NADH, NADH/ASA, GSH/ASA and GSH/NADH/ASA.

The reaction of the complexes **1–3** (approximately 1  $\mu\text{M}$ ) with NADH (80  $\mu\text{M}$ ) in 10% MeOH/90%  $\text{H}_2\text{O}$  (PBS, pH 7.4) was monitored by UV-Vis at r.t. after various time intervals. Turnover numbers (TON) were calculated from the difference in NADH concentration after 4 h divided by the concentration of complexes **1–3**. NADH concentration was obtained using an extinction coefficient  $\epsilon = 6220 \text{ M}^{-1} \text{ cm}^{-1}$ .<sup>11</sup> 80  $\mu\text{M}$  NADH in 10% MeOH/90% PBS in  $\text{H}_2\text{O}$  (pH 7.4) was analysed as a control.

Fluorescence spectroscopy was used to study the interaction of platinum complexes with BSA. Working solutions of **2** and **3** were prepared as MeOH/PBS in  $\text{H}_2\text{O}$  (1:10 v/v) solvent mixtures. A bovine serum albumin (BSA) stock solution was prepared in Tris buffer (5 mM Tris-HCl/10 mM NaCl at pH 7.2) and stored at 4 °C no more than 5 days before use. Solution of BSA (0.5  $\mu\text{M}$ ) was titrated with increasing concentration of the complexes (0–2.5  $\mu\text{M}$ ), and the fluorescence was measured. The possible fluorescence quenching mechanism can be interpreted using the classical Stern–Volmer equation (Eq. 1)

$$F_0/F = 1 + K_{sv}[Q] = 1 + K_q\tau_0[Q] \quad (1)$$

where  $F_0$  and  $F$  are the fluorescence intensities in the absence and presence of the metal complexes (Q), respectively;  $K_{sv}$  is the Stern–Volmer quenching constant, which can be obtained as the slope of  $F_0/F$  versus  $[Q]$ .

For comparative purposes, the hydrazo form of complex **3** was prepared by the reaction of **3** with an excess of ascorbic acid (5 molar equiv.) in 50% DMF/50%  $\text{H}_2\text{O}$  for 24 h (r.t.). After that, the reaction mixture, which changed the colour from orange to yellow, was evaporated to dryness and washed several times with water. Then the product was dried again and analysed by  $^1\text{H}$  NMR (50%  $\text{DMF-}d_7$ /50%  $\text{D}_2\text{O}$ ) and by mass spectrometry (in MeOH).

### Cyclic voltammetry

Voltammograms were obtained using 1 mM solutions (3 mL) of  $L^1$ ,  $L^2$  and **1–3** in 0.1 M acetonitrile solution of tetrabutylammonium perchlorate. All solutions were flushed by argon gas stream for at least 1 min. Instrumentation was connected in a three-electrode configuration using Pt auxiliary electrode, glassy carbon working electrode and  $\text{Ag}/\text{Ag}^+$  reference electrode. Glassy carbon electrode was cleaned on an alumina containing pad after every measurement to remove electrochemically deposited residues. Measuring range was

set from -2.5 to 2.5 V with initial polarity set to positive and scan rate to 100 mV/s for all samples except L<sup>1</sup> which had to be set to 50 mV/s to reliably reveal all half-waves. Ferrocene sample was also measured separately as a reference ( $E_{1/2}$  (ferrocene/ferrocenium) = 0.40 V)<sup>12</sup> and all values were corrected accordingly.

### **Cell culture and biochemicals**

Human prostate cancer DU-145 (ATCC HTB-81), human melanoma A375 (ATCC CRL-1619), human liver hepatocellular carcinoma HepG2 (ATCC HB-8065), human lung cancer A549 (ATCC CCL-185), and human breast cancer MCF-7 (ATCC HTB-22) cell lines, and culture media DMEM F-12HAM (Dulbecco's Modified Eagle Medium: Nutrient Mixture F-12), EMEM (Eagle's Minimum Essential Medium), DMEM (Dulbecco's Modified Eagle's Medium), and F-12K medium (Kaighn's Modification of Ham's F-12 Medium) were obtained from American Type Culture Collection (ATCC; Manassas, VA, USA). Foetal Bovine Serum (FBS) was purchased from Gibco (Waltham, MA, USA), whereas other biochemical reagents streptomycin/penicillin mixture, MTT (3-(4,5-dimethylthiazol-2-yl)-2,5-diphenyltetrazolium bromide) and cisplatin were supplied by Sigma–Aldrich (Darmstadt, Germany).

### ***In vitro* antiproliferative activity testing**

All cell lines were cultured in 5% CO<sub>2</sub> and fully humidified at 37 °C. The DU-145 cells were cultured in DMEM F-12HAM, HepG2 and MCF-7 cells in EMEM, A375 cells in DMEM, and A549 cells in F-12K medium. Media contained 10% FBS and antibiotics (1% streptomycin/penicillin mixture). Experiments were conducted in culture media with reduced content of FBS (2.5%).

MTT assay was applied to assess the viability of the cells. In brief, the cells were seeded in 96-well plates at an initial density of  $5 \times 10^3$  cells/well. Then, the cells were cultured in standard conditions for 24 h. Subsequently, the cells were treated with a medium containing increasing concentrations (0.1–25.0 μM) of complexes **1–3** (pre-dissolved in DMSO, 0.1% final concentration of DMSO) for 24 h. Next, 10 μL of MTT reagent was added to each well and the cells were incubated at 37 °C for additional 3 h. Then, by removing the medium, DMSO was added to each well to dissolve formazan crystals. The optical density (OD) data of converted dye was measured at 570 nm on a microplate reader (Spectra iD3 Max, Molecular Devices; San Jose, CA, USA). The reference drug cisplatin was included for comparative purposes. DMSO (0.1%) was used as a negative control. All experimental conditions were tested in triplicate and the experiment was done two times. Values represent mean percent of viability (in the percent of controls). Data of cell viability from the cytotoxicity assays were analysed using Mann–Whitney U test with GraphPad Prism 4.0 Software (GraphPad Software Inc., San Diego, CA, USA). Values of  $p < 0.05$  were considered to be statistically significant.

## Cellular accumulation

The A549 cells were seeded in 6-well culture plates at a density of  $1 \times 10^6$  cells per well and incubated overnight (37 °C and 5% CO<sub>2</sub> in a humidified incubator). Then, the cells were treated for 24 h by IC<sub>50</sub> concentrations of complexes **1–3**. Then the cells were washed with PBS (2 × 2 mL), harvested by the trypsinization, centrifuged and the obtained cell pellets were stored on ice. After that, the cells were digested in 500 µL of nitric acid (6 h, 70 °C), to give the fully homogenized solutions. The solutions were 1000× diluted with water and the metal content was determined by ICP-MS (*vide supra*). The obtained values were corrected for adsorption effects.

## Theoretical calculations

Theoretical calculations were done with ORCA 5.0 software.<sup>13,14</sup> The DFT calculations employed PBE0 hybrid functional<sup>15</sup> together with the atom-pairwise dispersion correction (D4).<sup>16</sup> The ZORA relativistic approximation<sup>17</sup> with SARC-ZORA-TZVP for Ru<sup>18</sup> and Ir,<sup>19</sup> ZORA-def2-TZVP(-f) for N, O, P, S, Cl and ZORA-def2-SVP for C and H atoms basis sets were employed.<sup>20</sup> The SARC/J Coulomb fitting basis set was utilized as an auxiliary basis set.<sup>21</sup> Also, chain-of-spheres (RIJCOSX) approximation to exact exchange was utilized.<sup>22,23</sup> Increased integration grids (defgrid3 in ORCA convention) and tight SCF convergence criteria were used in all calculations. Molecular geometries optimizations as well as frequency calculations for all studied complexes were performed without any symmetry restrictions and applying a conductor-like polarizable continuum model (CPCM) with the Gaussian charge scheme set for water.<sup>24,25</sup> The vibrational analyses confirmed proper convergence for complexes at local energy minimum (no imaginary frequencies) and in the case of the transition states geometries only one imaginary frequency was found corresponding to the correct movement of involved atoms. The thermochemistry data were calculated as implemented in ORCA at 298.15 K and Gibbs free energies were corrected by where the factor of 1.89 kcal/mol due to the change in standard state from gas phase to solution phase.<sup>26</sup> We considered separated reactants to define the energy reference state in order to predict the activation barriers. The nudged elastic band (NEB) method was also utilized to help in localization of the transition states.<sup>27</sup>

**Table S1.** Crystallographic data for **1–3**.

	<b>1</b>	<b>2·MeOH·H<sub>2</sub>O</b>	<b>3</b>
Formula	C <sub>28</sub> H <sub>27</sub> ClF <sub>6</sub> N <sub>5</sub> PRu	C <sub>30</sub> H <sub>38</sub> ClF <sub>6</sub> IrN <sub>5</sub> O <sub>3</sub> P	C <sub>28</sub> H <sub>28</sub> ClF <sub>6</sub> IrN <sub>5</sub> P
Formula weight	715.03	889.27	807.20
Crystal system	monoclinic	monoclinic	triclinic
Space group	<i>P</i> 2 <sub>1</sub> / <i>c</i>	<i>P</i> 2 <sub>1</sub> / <i>c</i>	<i>P</i> $\bar{1}$
Cell parameters			
<i>a</i> /Å	7.6846(2)	11.4394(3)	10.0327(8)
<i>b</i> /Å	31.8058(6)	11.8383(2)	12.7759(7)
<i>c</i> /Å	12.2255(4)	24.4773(6)	13.3366(8)
<i>α</i> /deg	90	90	106.522(5)
<i>β</i> /deg	105.629(2)	93.977(2)	107.084(5)
<i>γ</i> /deg	90	90	92.766(5)
<i>V</i> /Å <sup>3</sup>	2877.61(13)	3306.81(13)	1550.26(19)
<i>Z</i>	4	4	2
<i>T</i> /K	150.0(2)	100.0(2)	100.0(2)
Density, D <sub>c</sub> /g cm <sup>-3</sup>	1.650	1.786	1.729
Abs. coefficient/mm <sup>-1</sup>	6.395	9.678	10.180
Data	30076	41261	48750
R <sub>1</sub> <sup>a</sup> , wR <sub>2</sub> <sup>b</sup> [ <i>I</i> > 2σ( <i>I</i> )]	0.0706, 0.2185	0.0377, 0.0973	0.1161, 0.3217
Goodness of fit	1.095	1.083	1.137
CSD number	2055599	2055600	2055601

$$^a R_1 = \sum (|F_o| - |F_c|) / \sum |F_o|, \quad ^b wR_2 = \{\sum [w(F_o^2 - F_c^2)^2] / \sum [w(F_o^2)^2]\}^{1/2}$$

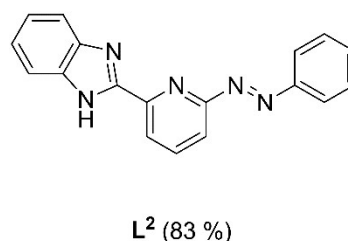
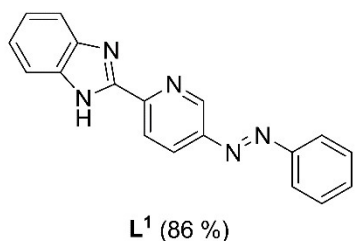
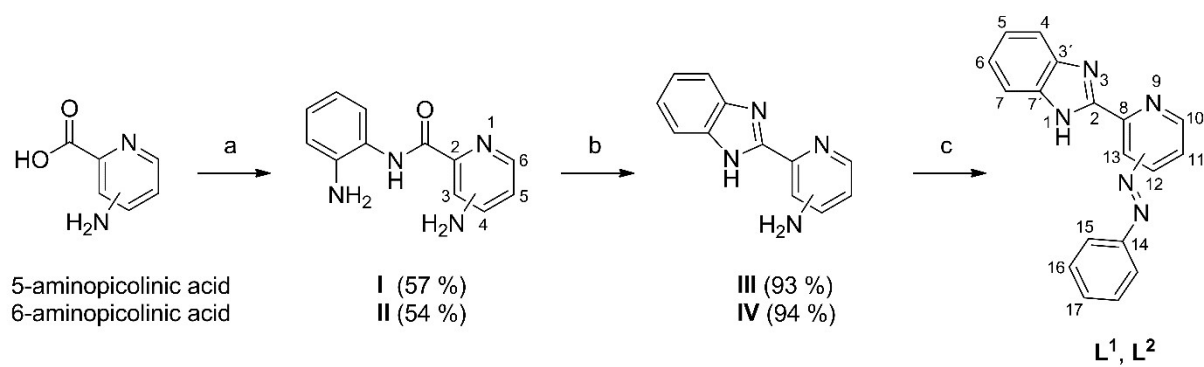
**Table S2.** Selected bond lengths (Å) and angles (°) determined for **1–3** by a single-crystal X-ray analysis.  $C_g$  = the centroid of the  $\eta$ -coordinated arene/arenyl ring (pcym for **1** and Cp\* for **2**·2MeOH·H<sub>2</sub>O and **3**), M = Ru for **1** and Ir for **2**·2MeOH·H<sub>2</sub>O and **3**.

	<b>1</b>	<b>2</b> ·2MeOH·H <sub>2</sub> O	<b>3</b>
<i>Bond</i>			
M–Cl1	2.404(1)	2.396(1)	2.401(3)
M–N1	2.108(5)	2.124(4)	2.197(13)
M–N2	2.087(5)	2.108(4)	2.124(11)
M– $C_g$	1.677(5)	1.784(4)	1.809(13)
<i>Angle</i>			
N1–M–N2	76.6(2)	76.1(2)	76.1(5)
N1–M–Cl1	84.1(1)	84.5(1)	88.7(3)
N1–M– $C_g$	131.2(2)	131.1(2)	132.8(5)
N2–M–Cl1	86.4(1)	86.8(1)	88.1(3)
N2–M– $C_g$	132.0(2)	134.0(2)	129.4(5)
Cl1–M– $C_g$	128.2(1)	126.3(1)	125.3(3)

**Table S3.** Selected structural parameters (Å, °) for hydrolysis of **1–3** calculated by DFT.<sup>a</sup>

[Ru( $\eta^6$ -pcym)Cl(L <sup>1</sup> )] <sup>+</sup> of <b>1</b>	R	TS	P
M-N <sub>py</sub>	2.096	2.122	2.097
M-N <sub>bim</sub>	2.069	2.079	2.068
M-C <sub>g</sub>	1.673	1.653	1.670
M-Cl	2.405	3.081	-
M-OH <sub>2</sub>	-	2.679	2.161
$\Delta G^\ddagger$		29.2	
[Ir( $\eta^5$ -Cp*)Cl(L <sup>1</sup> )] <sup>+</sup> of <b>2</b>	R	TS	P
M-N <sub>py</sub>	2.110	2.126	2.101
M-N <sub>bim</sub>	2.070	2.077	2.069
M-C <sub>g</sub>	1.769	1.749	1.762
M-Cl	2.406	3.158	-
M-OH <sub>2</sub>	-	2.696	2.191
$\Delta G^\ddagger$		27.0	
[Ir( $\eta^5$ -Cp*)Cl(L <sup>2</sup> )] <sup>+</sup> of <b>3</b>	R	TS	P
M-N <sub>py</sub>	2.128	2.125	2.113
M-N <sub>bim</sub>	2.062	2.052	2.068
M-C <sub>g</sub>	1.774	1.769	1.763
M-Cl	2.413	3.283	-
M-OH <sub>2</sub>	-	2.974	2.179
$\Delta G^\ddagger$		30.5	

<sup>a</sup> N<sub>py</sub> is nitrogen donor atom of pyridine part of L<sup>1</sup>/L<sup>2</sup>; N<sub>bim</sub> is nitrogen donor atom of benzimidazole part of L<sup>1</sup>/L<sup>2</sup>; unit of  $\Delta G^\ddagger$  are kcal/mol.



**Scheme S1.** Synthesis of phenylazo pybzim ligands L<sup>1</sup> and L<sup>2</sup>: Reaction conditions: (a) *o*-phenylenediamine, TBTU, DIPEA, DMF, r.t., 22–25 h; (b) AcOH, 100 °C, 1 h; (c) nitrosobenzene, 50% aq. NaOH, TBAB, pyridine, 50 °C, 3.5–5 h.

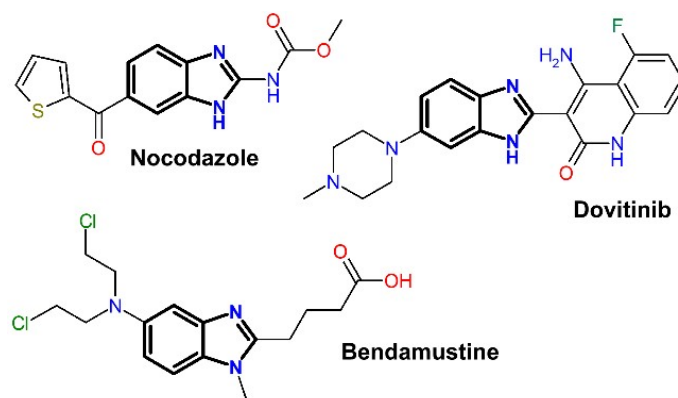


**Figure S1.** Structural formulas of selected anticancer benzimidazole derivatives.

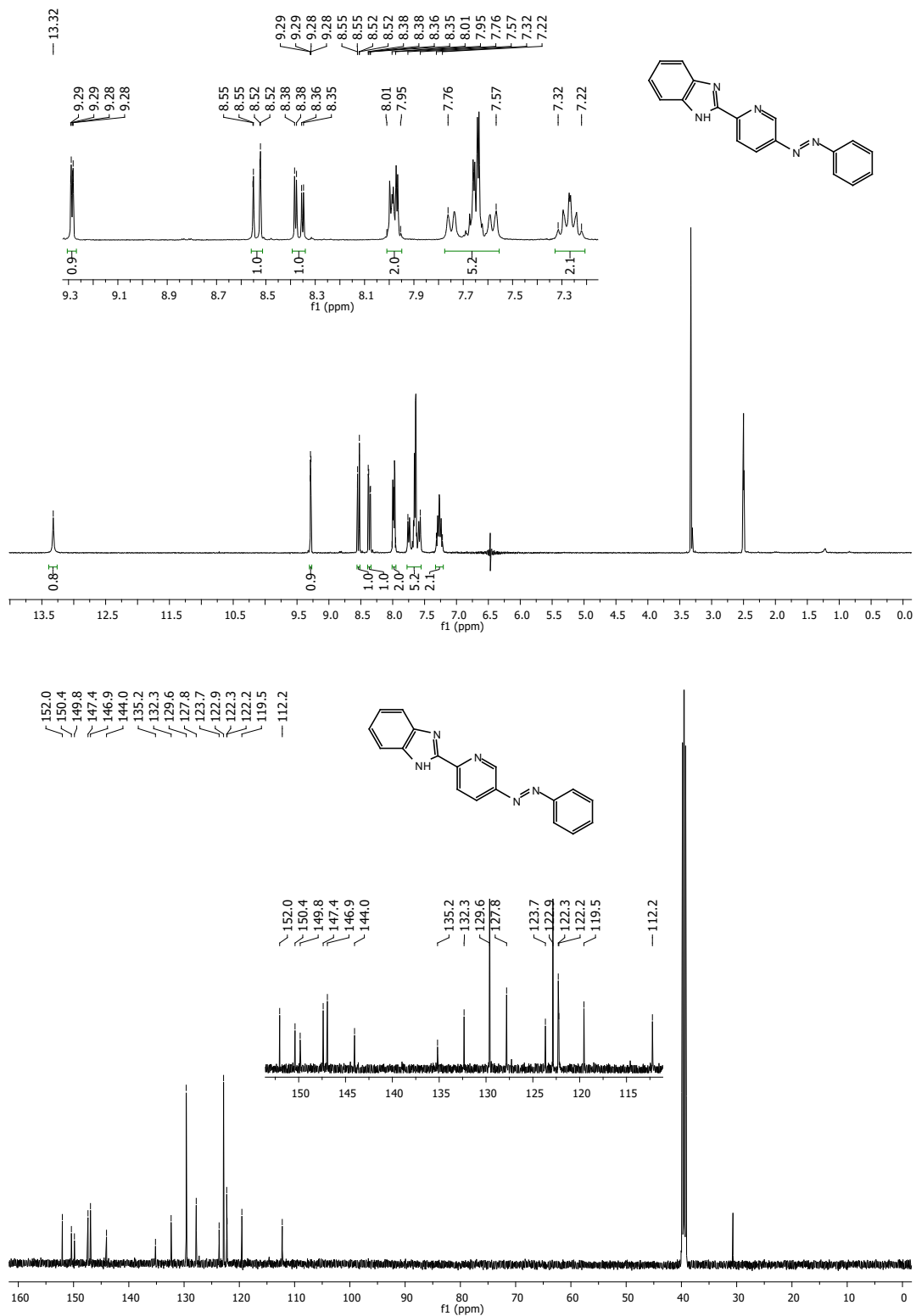


**Figure S2.** <sup>1</sup>H (top) and <sup>13</sup>C (bottom) NMR spectra of compound L<sup>1</sup> (dissolved in DMSO-*d*<sub>6</sub>).

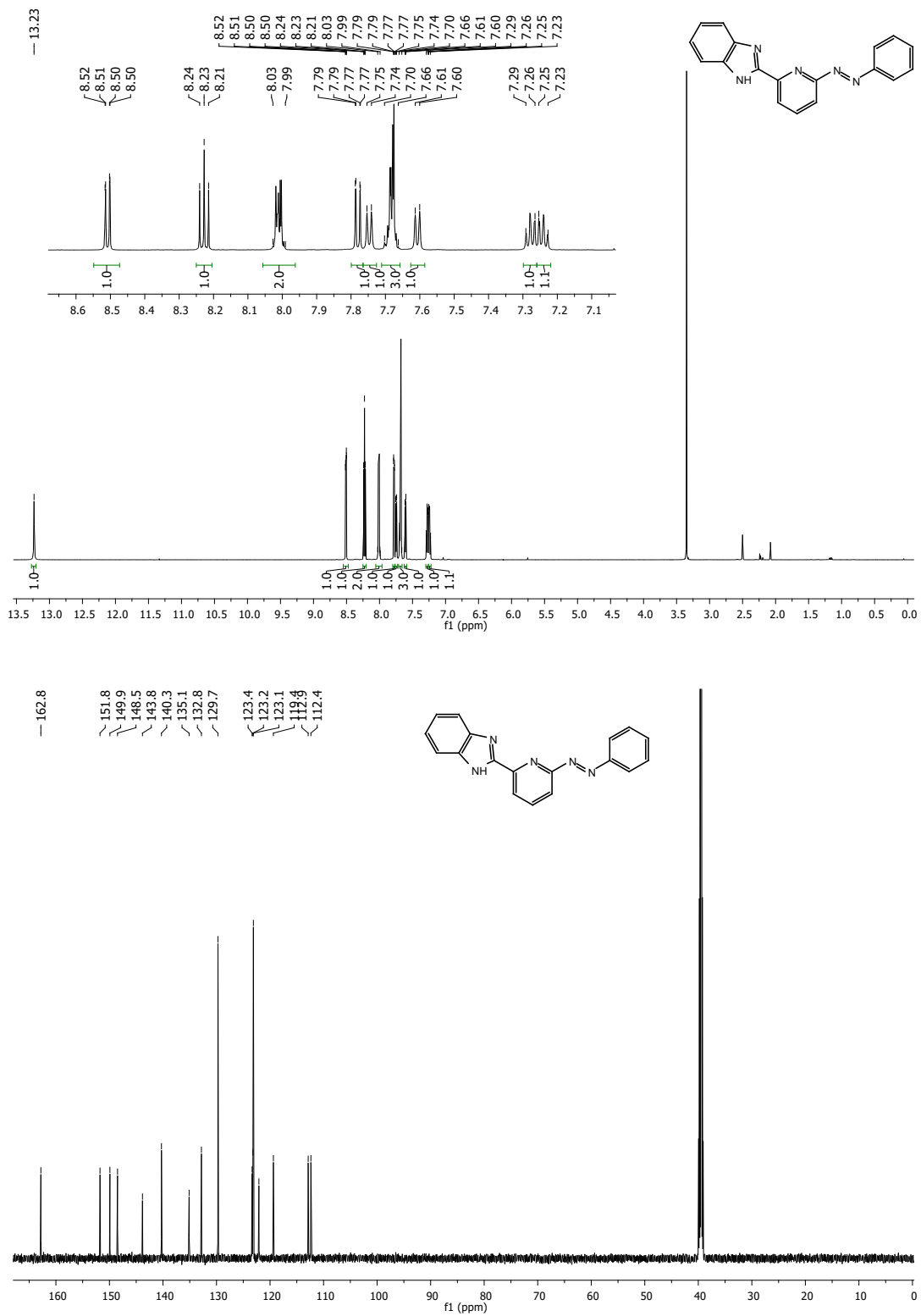


**Figure S3.** <sup>1</sup>H (top) and <sup>13</sup>C (bottom) NMR spectra of compound L<sup>2</sup> (dissolved in DMSO-*d*<sub>6</sub>).

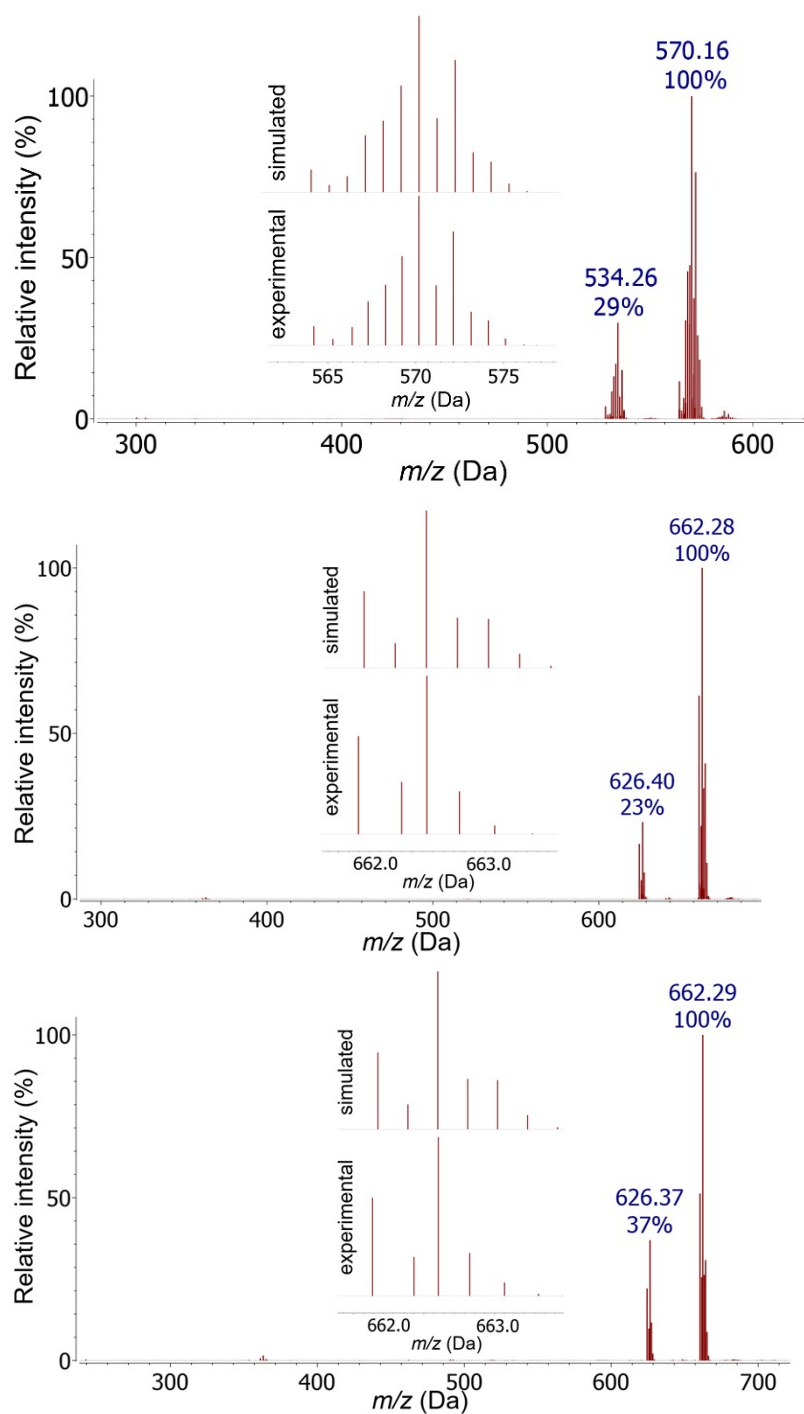


**Figure S4.** ESI+ mass spectra of complexes **1-3** (dissolved in MeOH), given with details of both the experimental (*inset bottom*) and simulated (*inset top*) isotopic pattern of the  $[M(ar)Cl(L^n)]^+$  species; ESI+ = positive electrospray ionization mode.

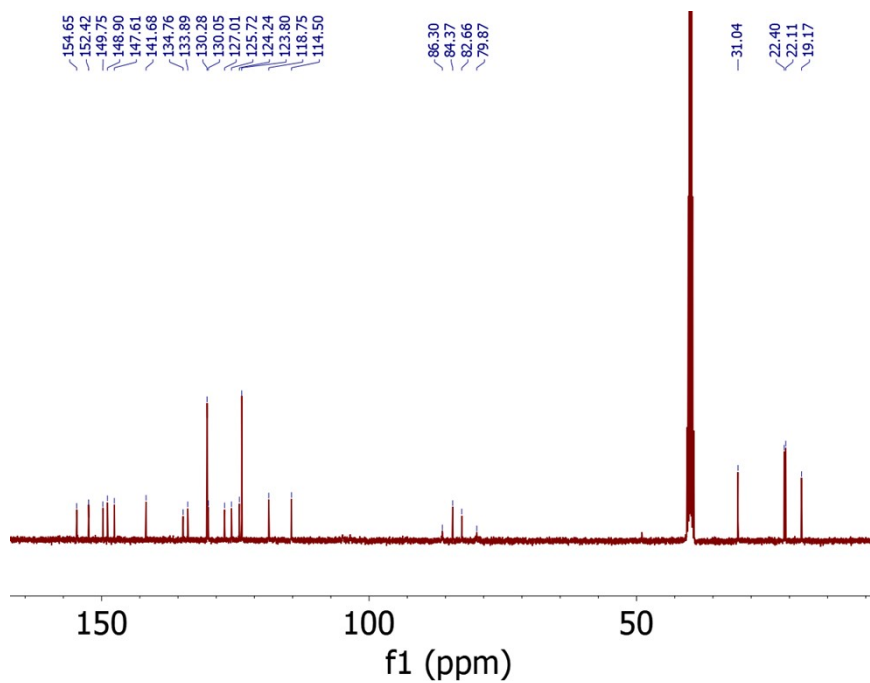
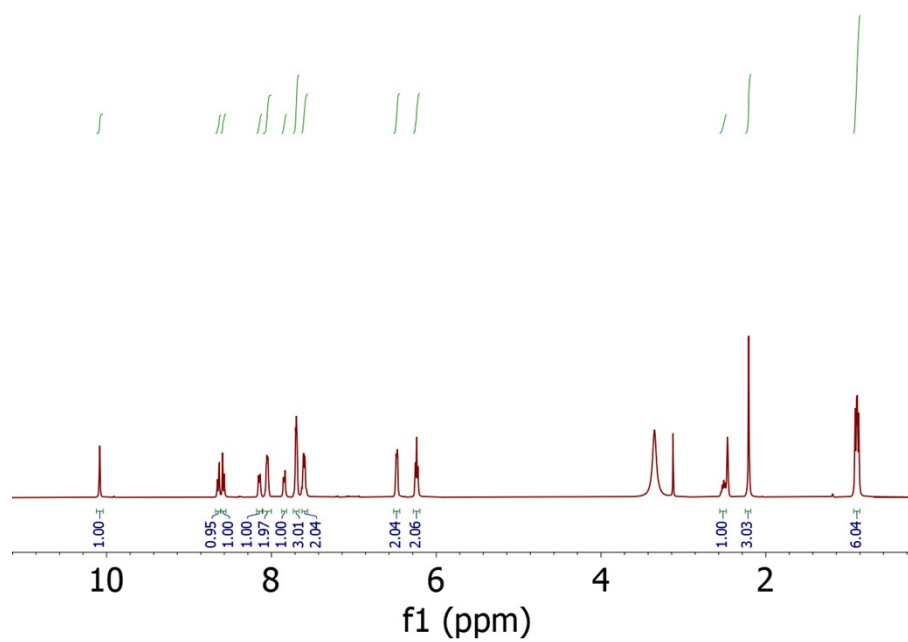


**Figure S5.**  $^1\text{H}$  (top) and  $^{13}\text{C}$  (bottom) NMR spectrum of complex **1** in  $\text{DMSO-}d_6$ .

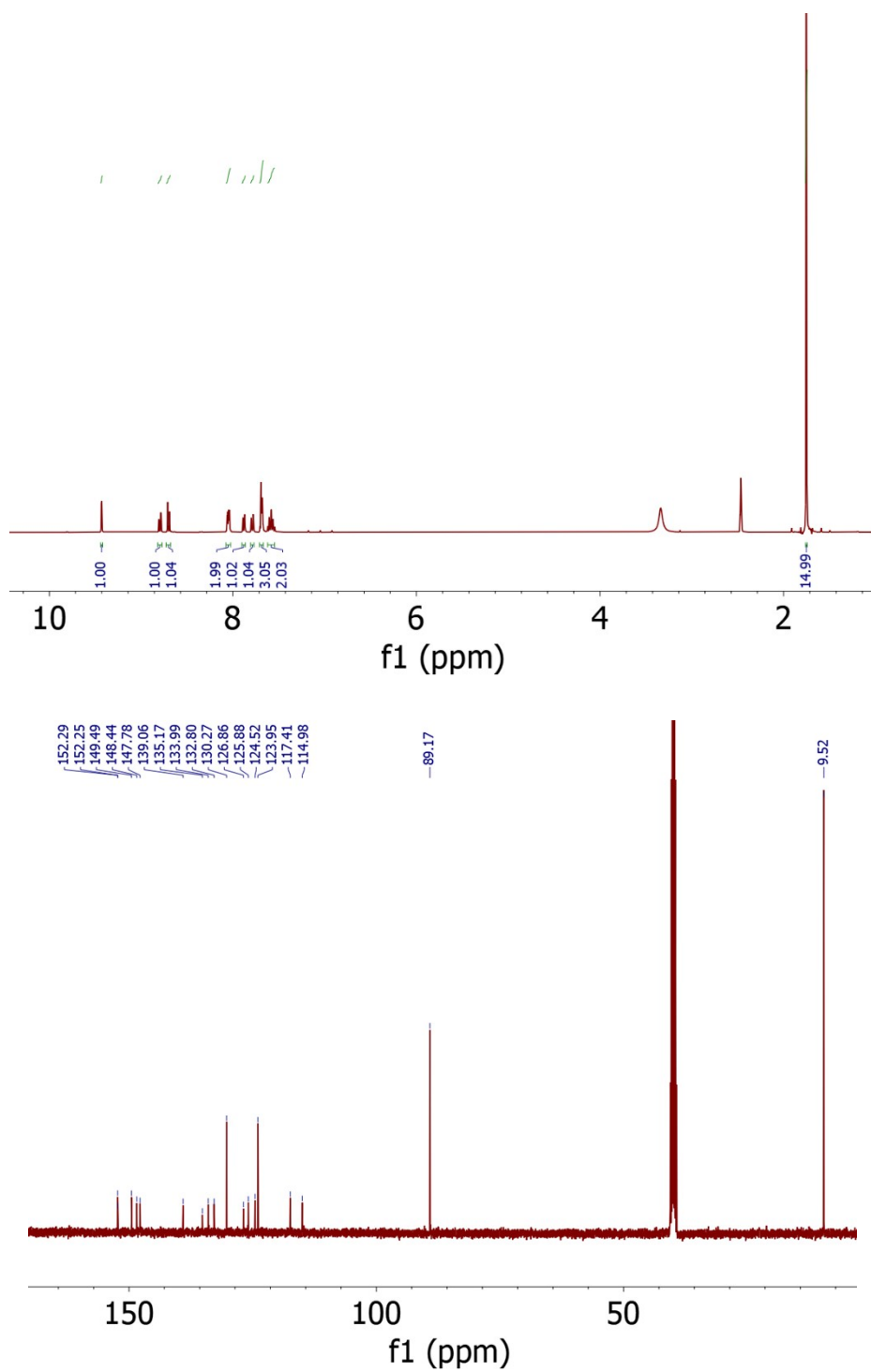


**Figure S6.**  $^1\text{H}$  (top) and  $^{13}\text{C}$  (bottom) NMR spectrum of complex 2 in  $\text{DMSO-}d_6$ .

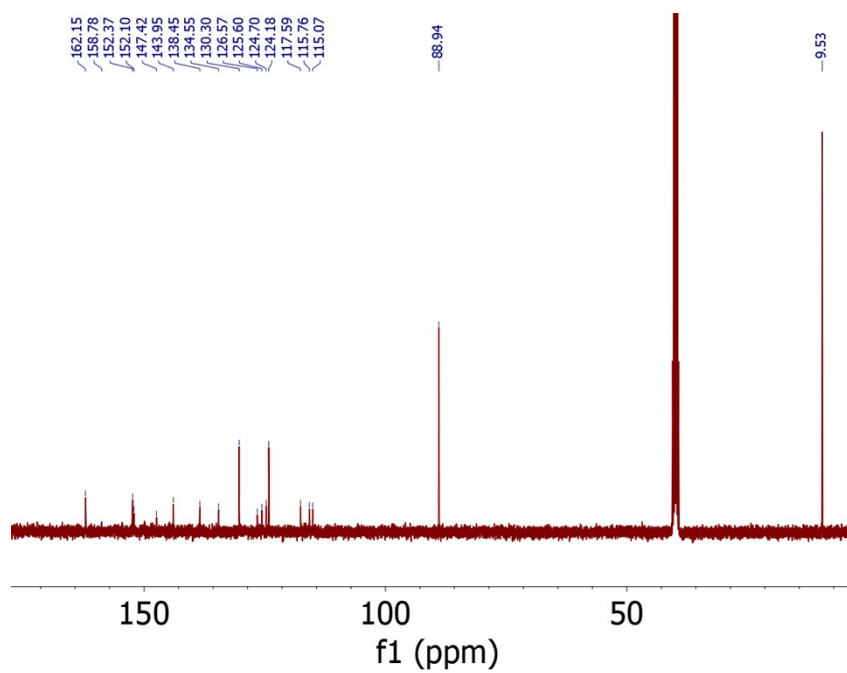
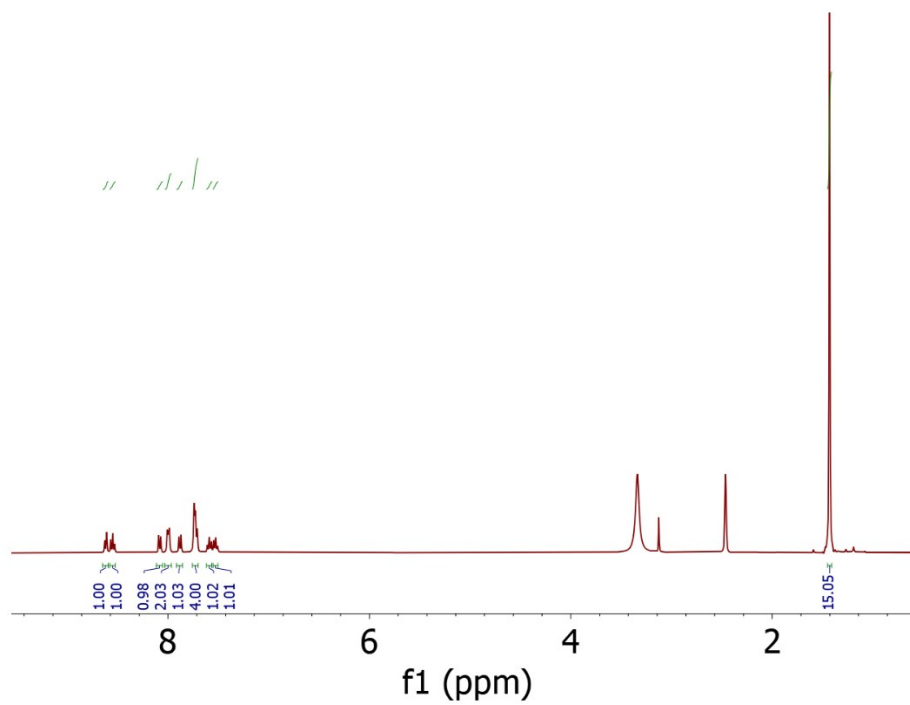


**Figure S7.**  $^1\text{H}$  (*top*) and  $^{13}\text{C}$  (*bottom*) NMR spectrum of complex **3** in  $\text{DMSO-}d_6$ .

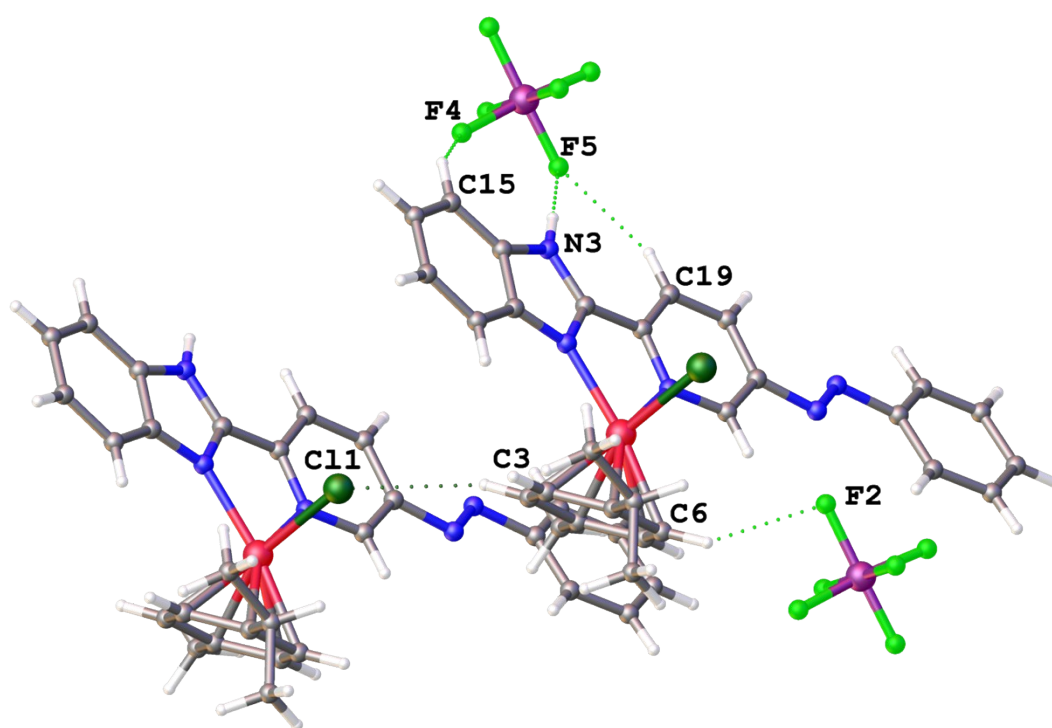
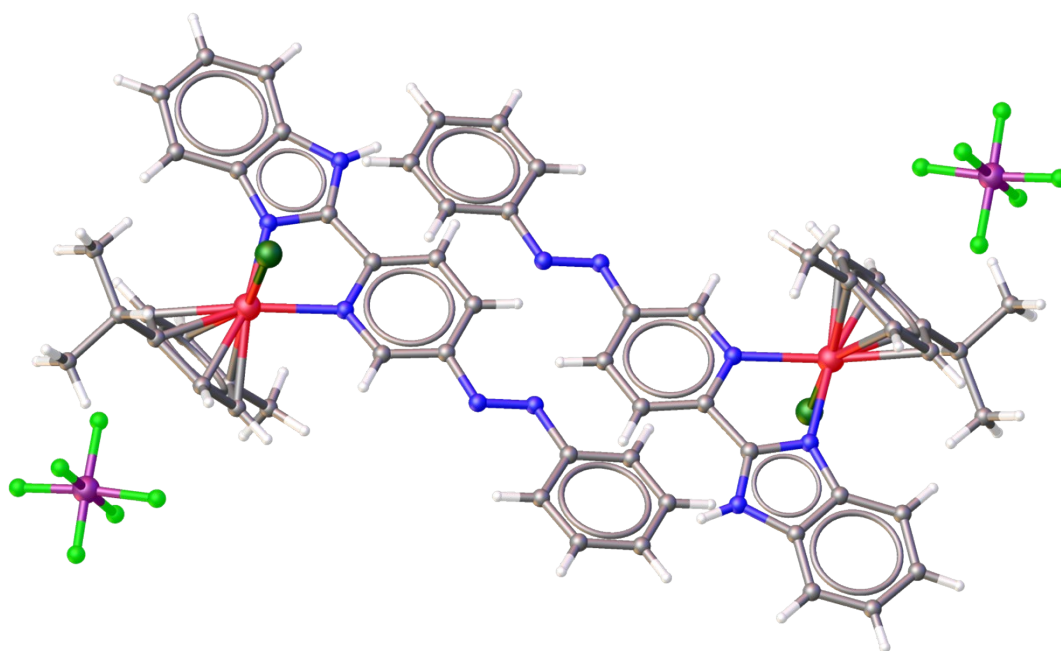


**Figure S8.** The  $\pi$ - $\pi$  stacking (*top*) and N-H $\cdots$ F, C-H $\cdots$ F and C-H $\cdots$ Cl (*bottom*) non-covalent interactions of complex **1**. Dihedral angles equal  $7.4^\circ$  (between the pyridine ring and 1*H*-benzimidazole moiety) and  $56.2^\circ$  (between the plane formed by the atoms of the five-membered RuN<sub>2</sub>C<sub>2</sub> chelate ring).

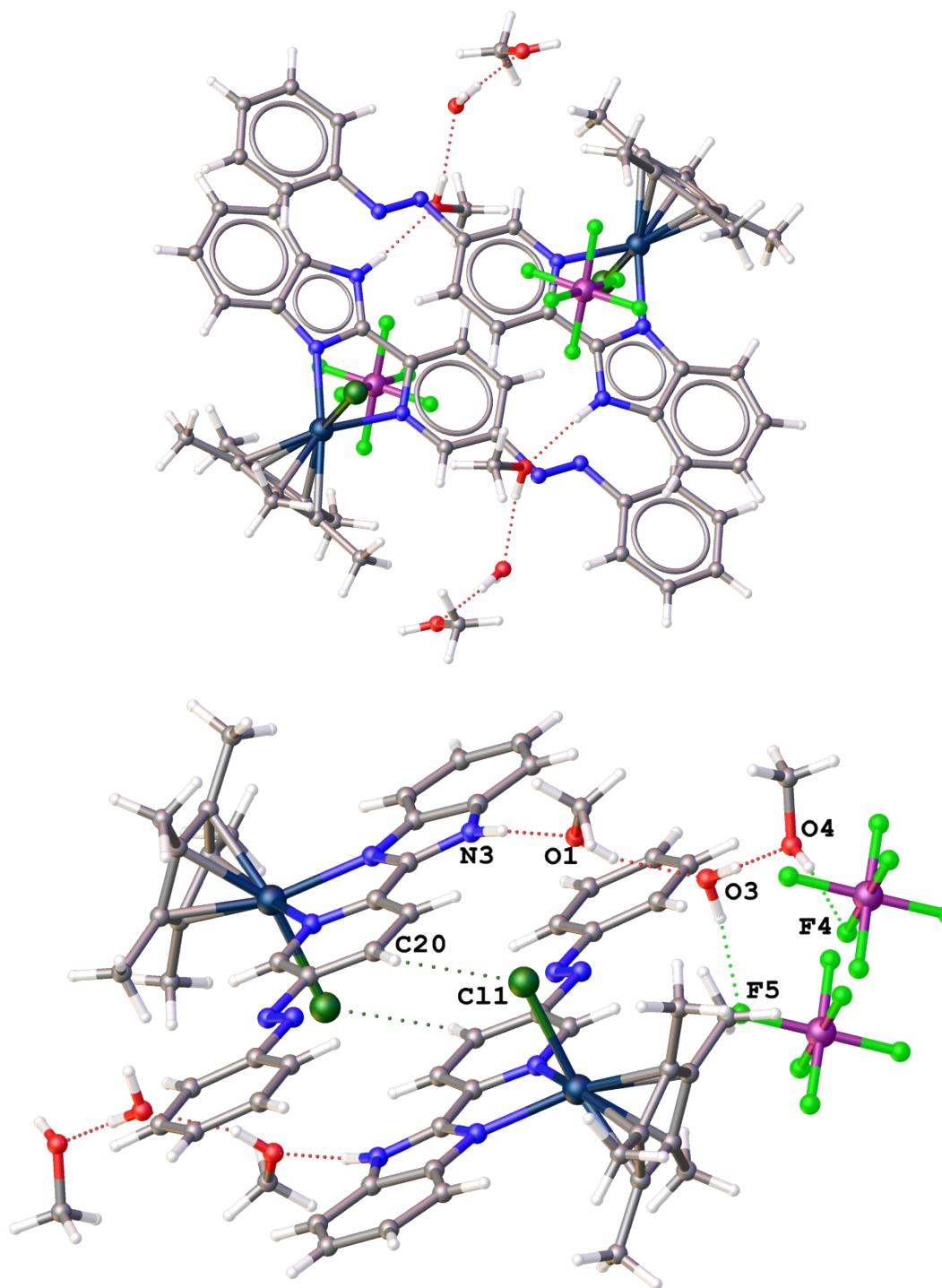


**Figure S9.** The  $\pi$ - $\pi$  stacking interactions and N-H $\cdots$ O and O-H $\cdots$ O hydrogen bonds (*top*), and N-H $\cdots$ O, O-H $\cdots$ O, O-H $\cdots$ F and C-H $\cdots$ Cl non-covalent interactions (*bottom*) of complex 2·2MeOH·H<sub>2</sub>O. Dihedral angles equal 2.9° (between the pyridine ring and 1*H*-benzimidazole moiety) and 57.5° (between the plane formed by the atoms of the five-membered IrN<sub>2</sub>C<sub>2</sub> chelate ring).

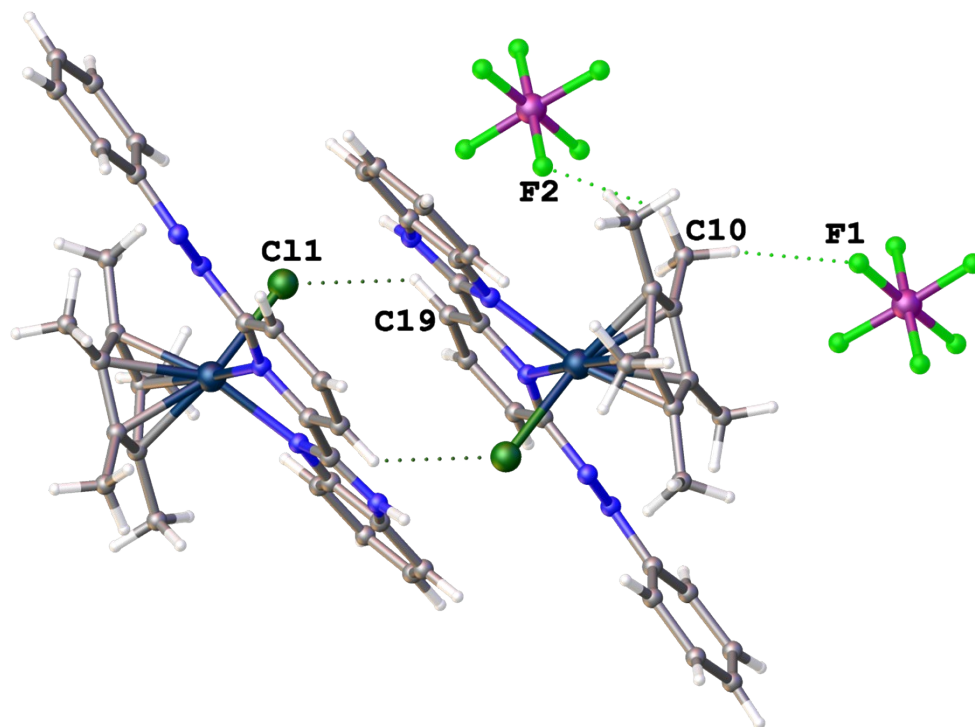


**Figure S10.** The C–H···F and C–H···Cl non-covalent interactions of complex **3**. Dihedral angles equal  $10.4^\circ$  (between the pyridine ring and 1*H*-benzimidazole moiety) and  $49.9^\circ$  (between the plane formed by the atoms of the five-membered IrN<sub>2</sub>C<sub>2</sub> chelate ring).

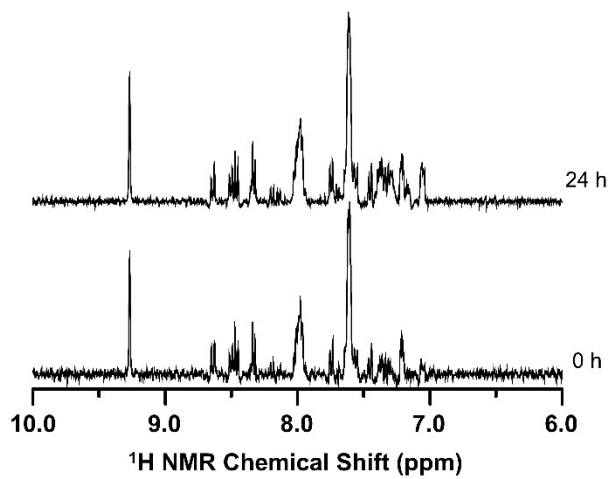
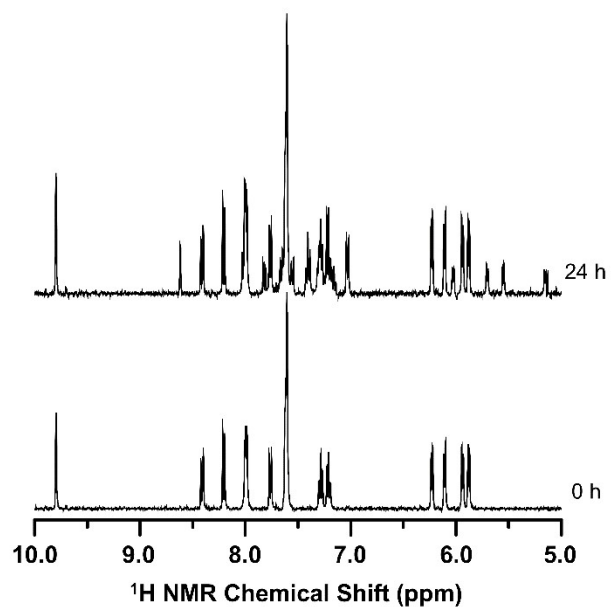


**Figure S11.** <sup>1</sup>H NMR studies of complex **1** (*top*) and **2** (*bottom*) in 50% DMSO-*d*<sub>6</sub>/50% PBS in D<sub>2</sub>O, as observed at different time points (0 h and 24 h).

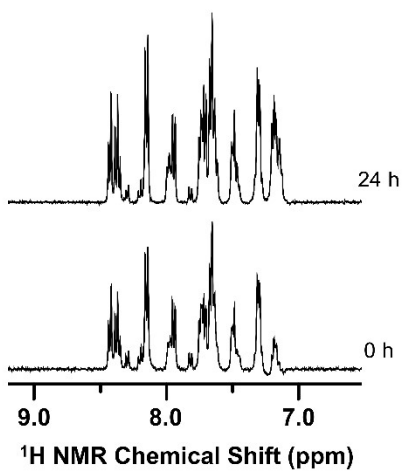
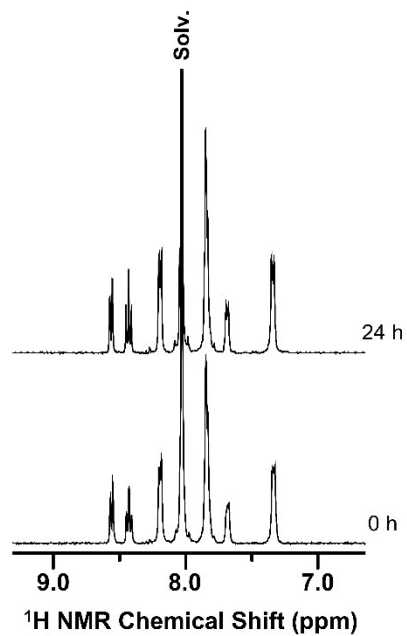


**Figure S12.**  $^1\text{H}$  NMR studies of complex **3** in 50%  $\text{DMF-}d_7$ /50% PBS in  $\text{D}_2\text{O}$  (*top*) and 50%  $\text{DMSO-}d_6$ /50% PBS in  $\text{D}_2\text{O}$  (*bottom*), as observed at different time points (0 h and 24 h).  
Solv =  $\text{DMF-}d_7$ .

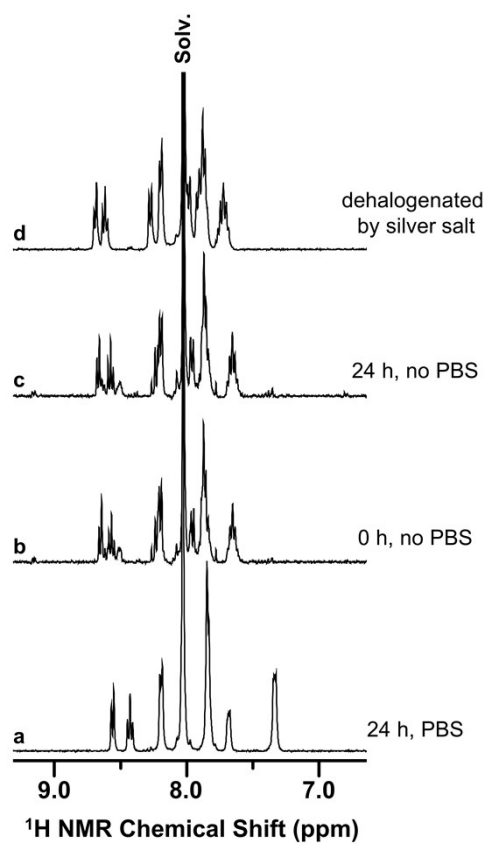


**Figure S13.** <sup>1</sup>H NMR studies of complex **3** in 50% DMF-*d*<sub>7</sub>/50% PBS in D<sub>2</sub>O (*a*) and 50% DMF-*d*<sub>7</sub>/50% D<sub>2</sub>O (*b*, *c*) at different time points (*t* = 0 h for *b*, and *t* = 24 h for *a* and *c*). The spectrum of **3** dissolved in 50% DMF-*d*<sub>7</sub>/50% D<sub>2</sub>O and dehalogenated by a stoichiometric amount of AgNO<sub>3</sub> is given for comparative purposes. Solv = DMF-*d*<sub>7</sub>.

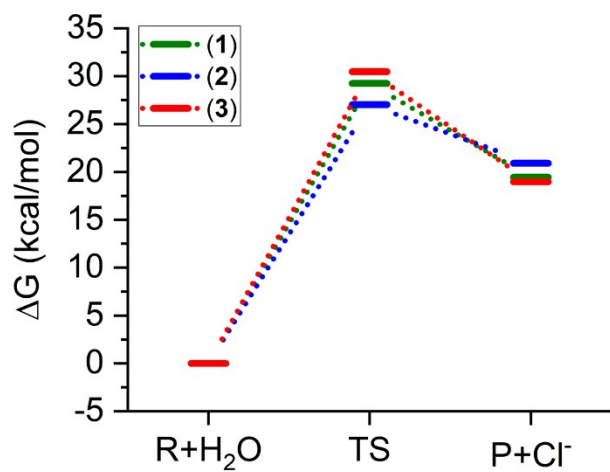


**Figure S14.** Relative Gibbs free energies of the reactants (R), transition states (TS) and products (P) for hydrolysis of [Ru(η<sup>6</sup>-pym)Cl(L<sup>1</sup>)]<sup>+</sup> of **1**, [Ir(η<sup>5</sup>-Cp\*)Cl(L<sup>1</sup>)]<sup>+</sup> of **2** and [Ir(η<sup>5</sup>-Cp\*)Cl(L<sup>2</sup>)]<sup>+</sup> of **3**.

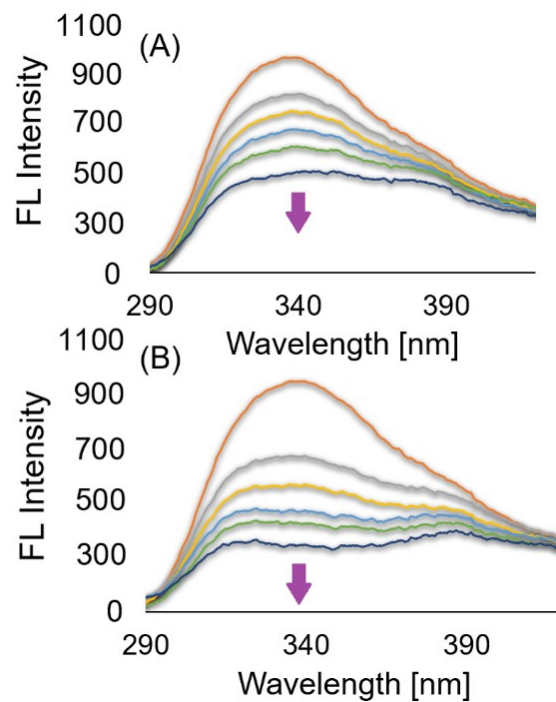


**Figure S15.** Fluorescence spectra of bovine serum albumin ( $c_{\text{BSA}} = 0.5 \mu\text{M}$ ) in the absence (orange colour) and presence of complexes **2** and **3** (0–2.5  $\mu\text{M}$  concentrations). The arrow shows the intensity changes with increasing concentration of complexes.

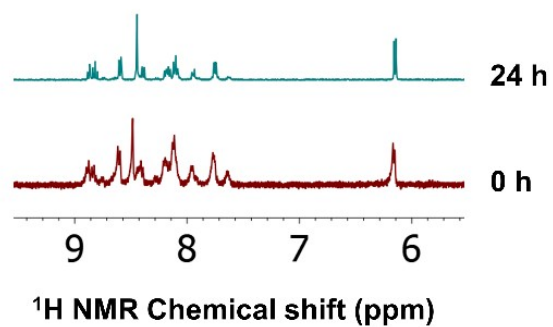


**Figure S16.** <sup>1</sup>H NMR studies of complex **3** in 50% DMSO-*d*<sub>6</sub>/50% PBS in D<sub>2</sub>O (pH 7.4) with 5 molar equiv. of GMP, as observed at different time points (0 h or 24 h).

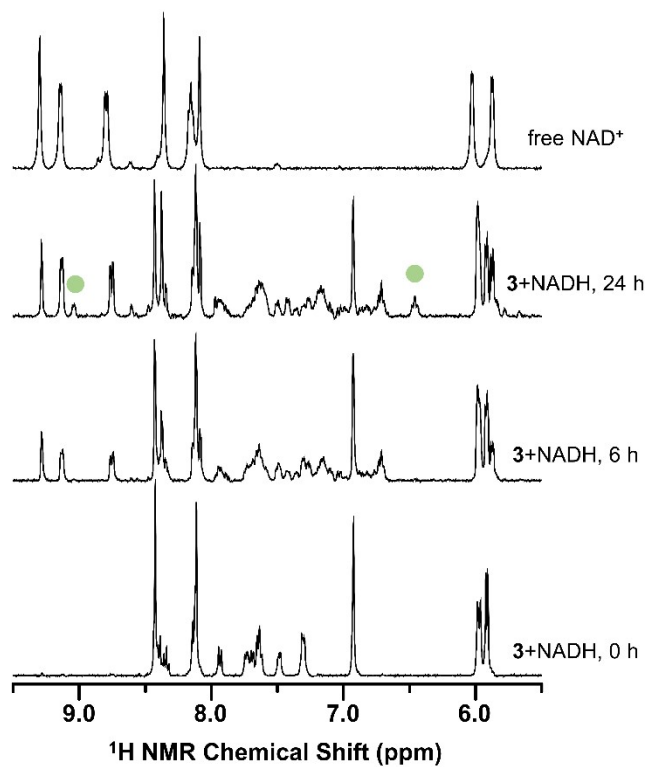


**Figure S17.**  $^1\text{H}$  NMR studies of complex **3** in 50% DMSO- $d_6$ /50% PBS in  $\text{D}_2\text{O}$  (pH 7.4) + 5 molar equivalents of NADH, as observed at different time points (0 h and 6 h). The  $^1\text{H}$  NMR spectrum of free NAD<sup>+</sup> in the same medium is given for comparative purposes. Green spheres - unidentified signals.

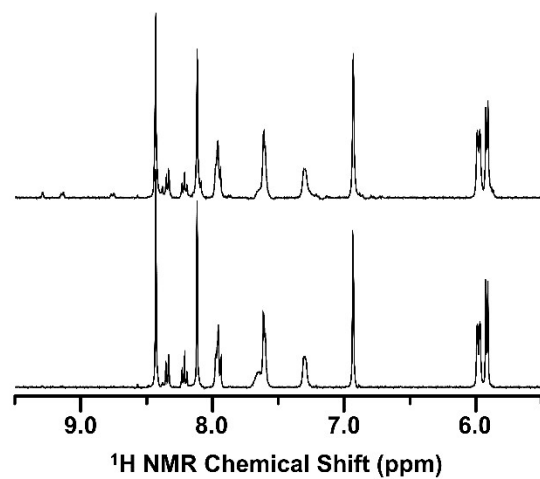


**Figure S18.**  $^1\text{H}$  NMR studies (control experiment) of L2 in 50%  $\text{DMSO-}d_6$ /50% PBS in  $\text{D}_2\text{O}$  (pH 7.4) + 5 molar equivalents of NADH, as observed at  $t = 0$  h (*bottom*) and  $t = 24$  h (*top*).

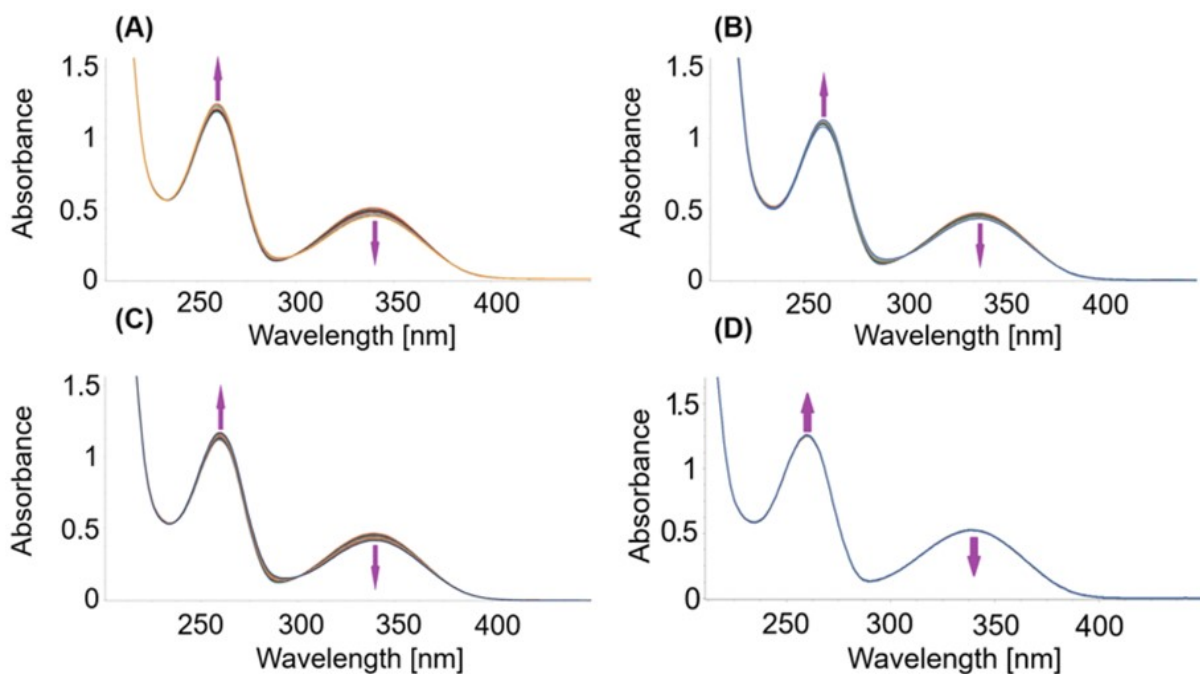


**Figure S19.** UV/Vis spectra of the reaction of NADH (80  $\mu\text{M}$ ) with 1  $\mu\text{M}$  complexes **1** (A), **2** (B) and **3** (C), studied at 298 K for 4 h. The control experiment with only NADH (80  $\mu\text{M}$ , same experimental conditions) is given for comparative purposes (D).

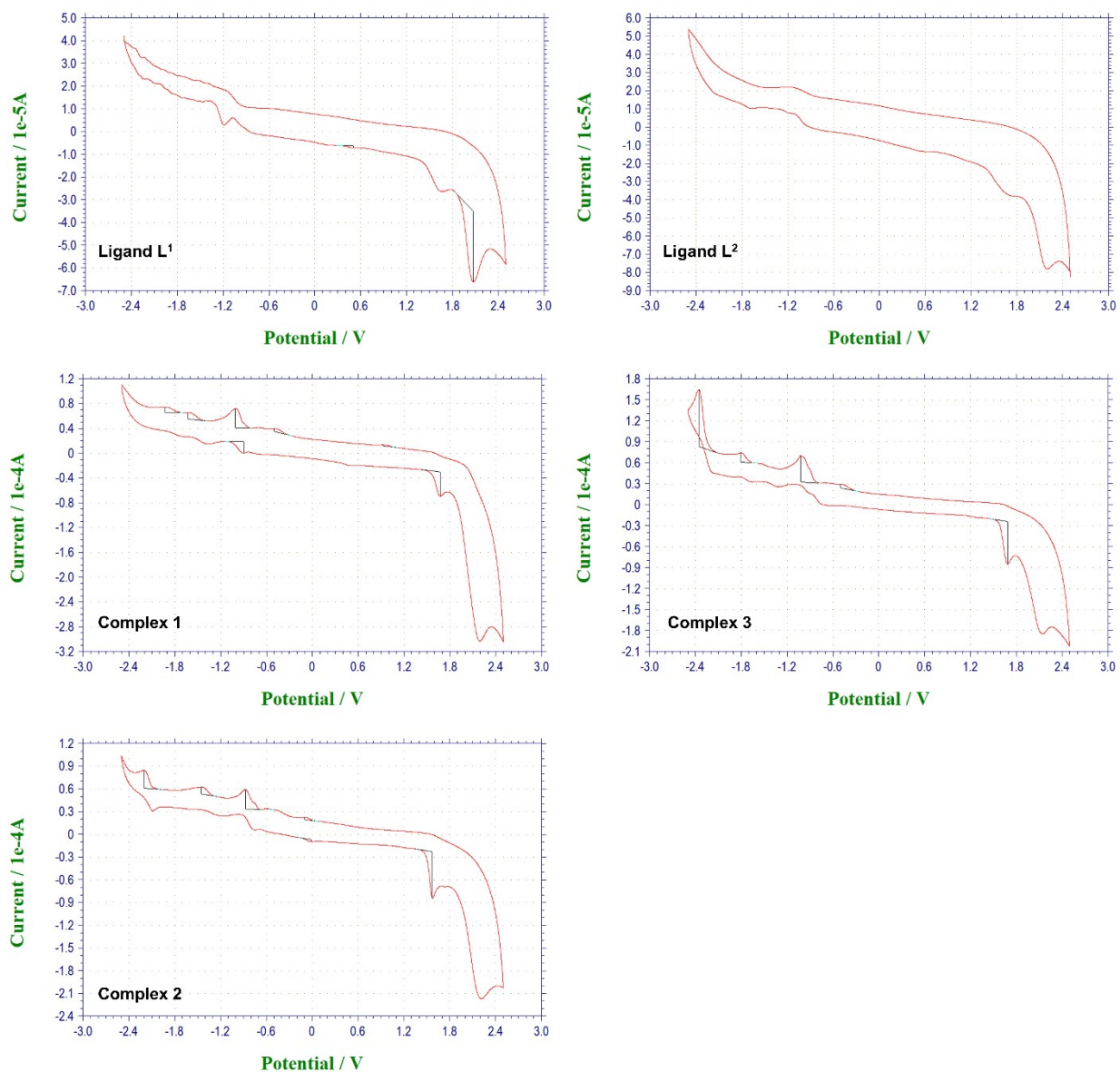


**Figure S20.** Cyclic voltammograms of ligands L<sup>1</sup> and L<sup>2</sup> and complexes 1–3 in 0.1 M (Bu<sub>4</sub>N)PF<sub>6</sub> in acetonitrile. Scan rate was 50 mV/s. The experiments were performed repeatedly with similar results obtained.

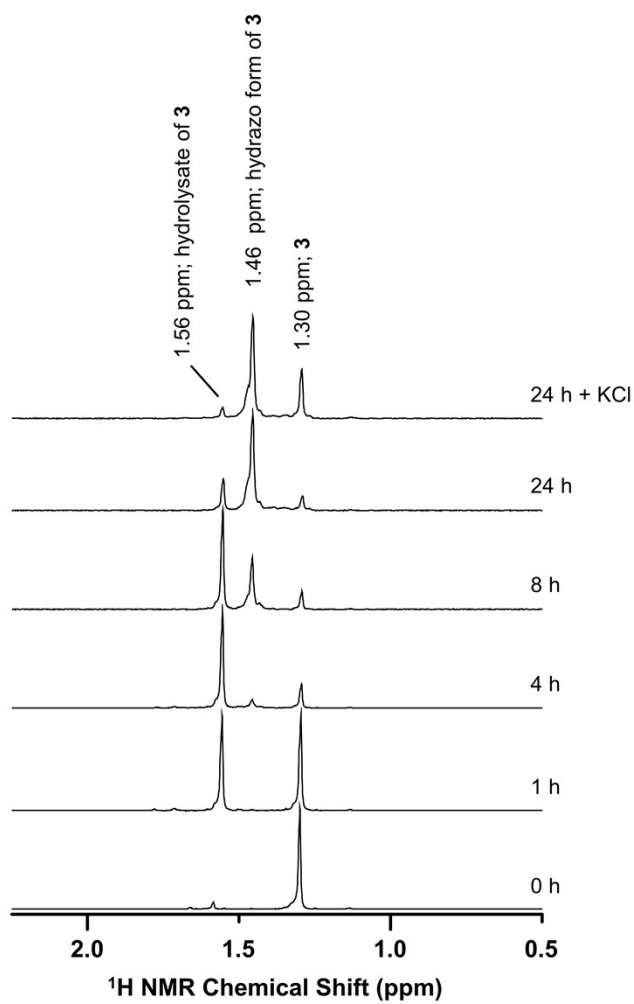


**Figure S21.**  $^1\text{H}$  NMR studies of complex **3** in 50% DMSO- $d_6$ /50% PBS in  $\text{D}_2\text{O}$  (pH 7.4) + 5 molar equivalents of NADH, as observed at different time points.

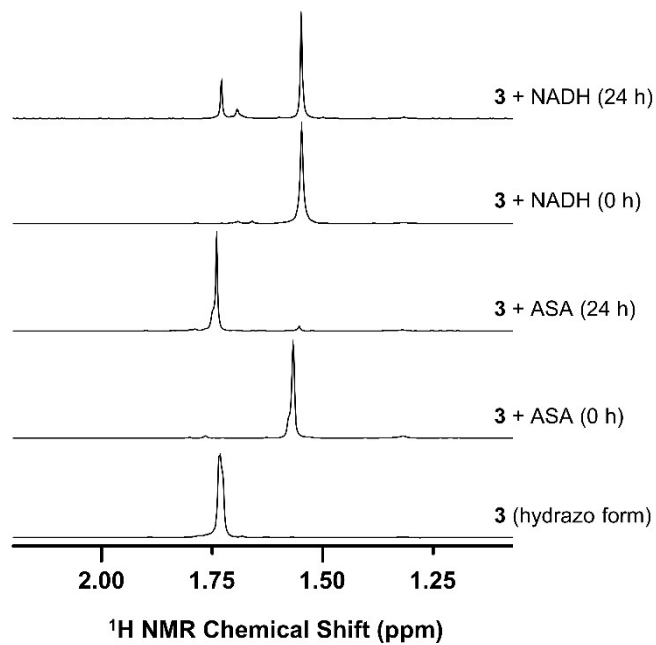


**Figure S22.** The results of <sup>1</sup>H NMR of the synthetic hydrazo form of complex **3** (dissolved in 50% DMF-*d*<sub>7</sub>/50% D<sub>2</sub>O), given with the spectra recorded on the mixtures of **3** with ascorbic acid (ASA) or reduced nicotinamide adenine dinucleotide (NADH) in the same medium.

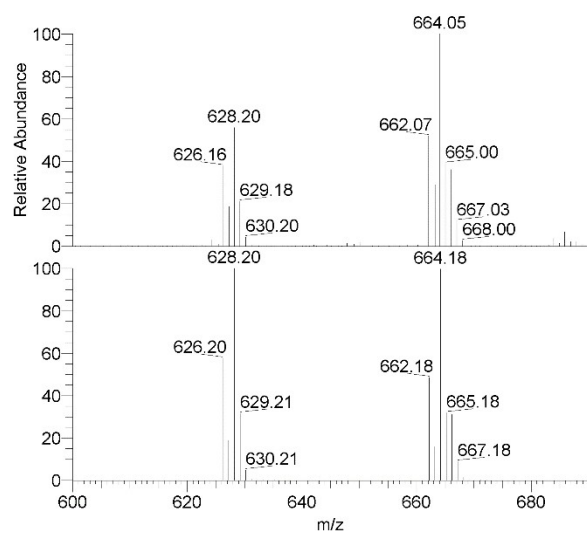
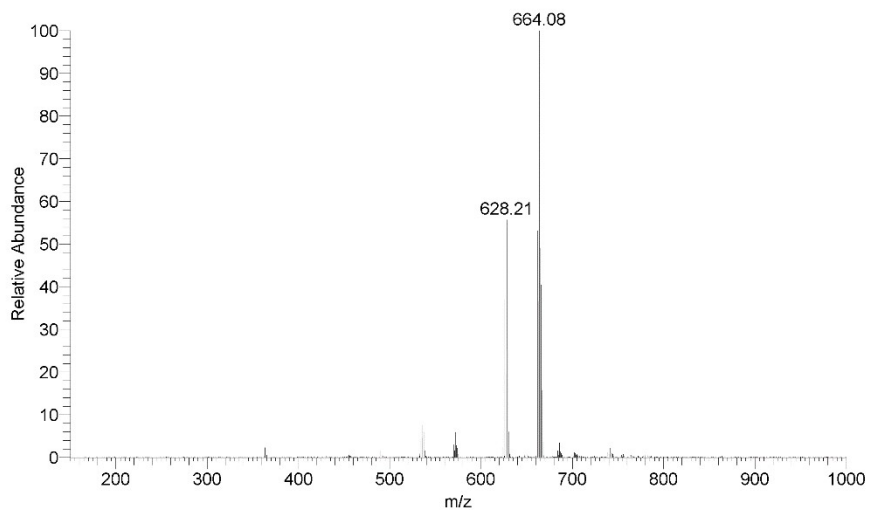


**Figure S23.** The results of ESI+ mass spectrometry of the synthetic hydrazo form of complex **3** (dissolved in MeOH). The detected signals are assignable to  $\{[\text{IrCl}(\text{Cp}^*)(\text{L}^2)]+2\text{H}\}^+$  (hydrazo form of **3**; 664.1  $m/z$ ) and  $\{[\text{Ir}(\text{Cp}^*)(\text{L}^2)]+\text{H}\}^+$  (dehydrochlorinated hydrazo form of **3**; 628.2  $m/z$ ).

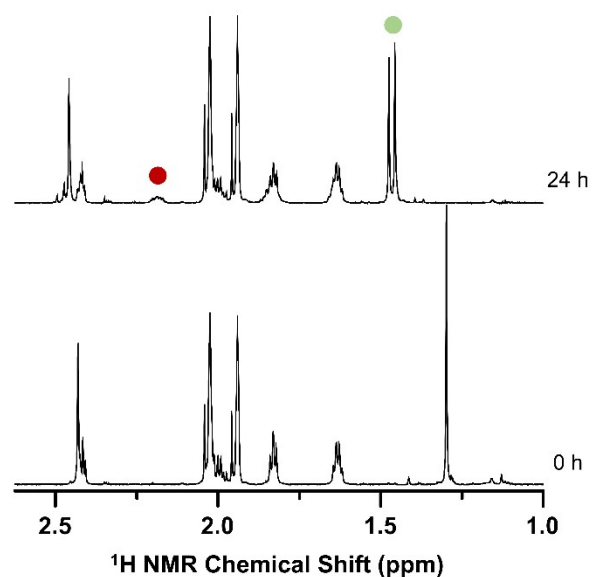


**Figure S24.** <sup>1</sup>H NMR studies of complex **3** in 50% DMF-*d*<sub>7</sub>/50% PBS in D<sub>2</sub>O (pH 7.4) with 5 molar equiv. of GSH, as observed at different time points (0 h or 24 h). Red sphere indicates one of two β-CH<sub>2</sub> resonances of [Ir<sub>2</sub>(η<sup>5</sup>-Cp\*)<sub>2</sub>(μ-SG)<sub>3</sub>]<sup>+</sup> and GSSG, and green sphere indicates the Cp\* resonance of the dinuclear [Ir<sub>2</sub>(η<sup>5</sup>-Cp\*)<sub>2</sub>(μ-SG)<sub>3</sub>]<sup>+</sup> species.

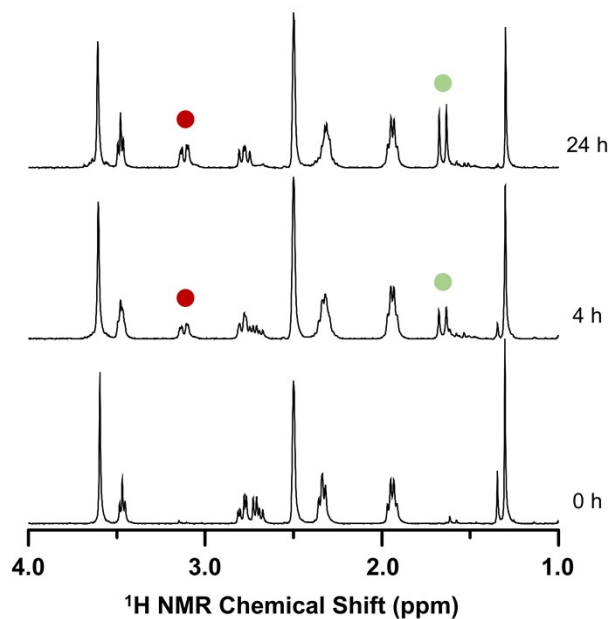


**Figure S25.** <sup>1</sup>H NMR studies of complex **3** in 50% DMSO-*d*<sub>6</sub>/50% PBS in D<sub>2</sub>O (pH 7.4) with 5 molar equiv. of GSH, as observed at different time points (0, 4 or 24 h) under inert atmospheres (N<sub>2</sub>). Red sphere indicates one of two β-CH<sub>2</sub> resonances of [Ir<sub>2</sub>(η<sup>5</sup>-Cp\*)<sub>2</sub>(μ-SG)<sub>3</sub>]<sup>+</sup> and GSSG, and green sphere indicates the Cp\* resonance of the dinuclear [Ir<sub>2</sub>(η<sup>5</sup>-Cp\*)<sub>2</sub>(μ-SG)<sub>3</sub>]<sup>+</sup> species.

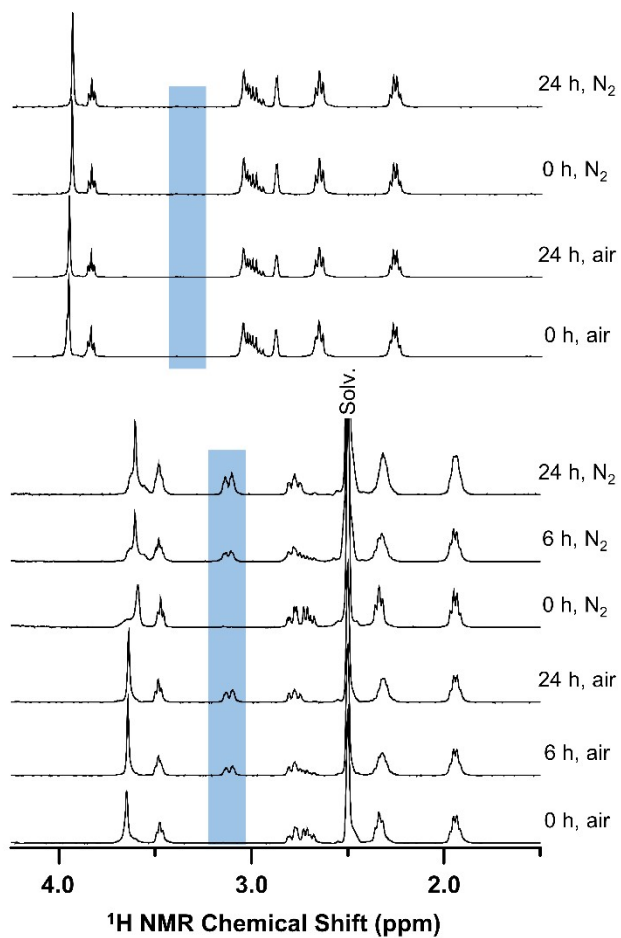


**Figure S26.** <sup>1</sup>H NMR studies of stability of the reduced glutathione (GSH) in the mixture of 50% DMF-*d*<sub>7</sub>/50% PBS in D<sub>2</sub>O (pH 7.4) (*top*) and 50% DMSO-*d*<sub>6</sub>/50% PBS in D<sub>2</sub>O (pH 7.4) (*bottom*), as observed at different time points under air or nitrogen atmosphere. Blue regions indicate β-CH<sub>2</sub> resonances of GSSG.

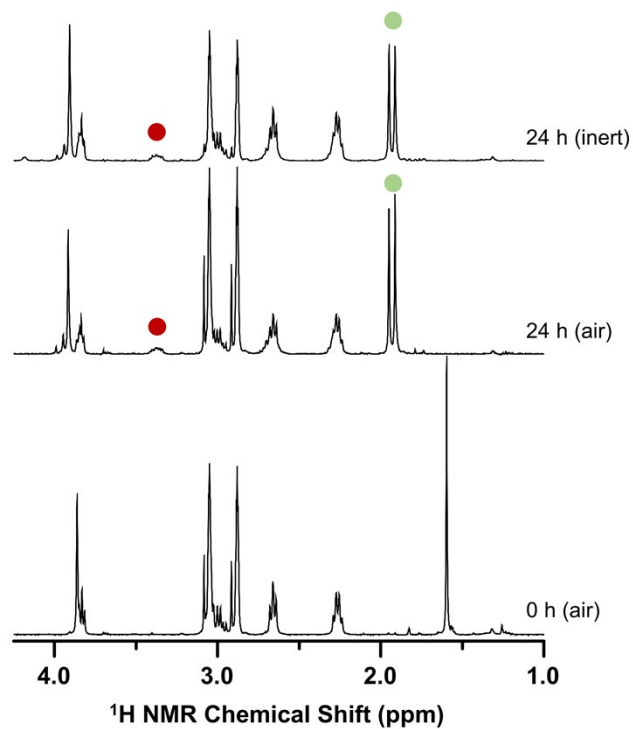


**Figure S27.** <sup>1</sup>H NMR studies of complex **3** in 50% DMF-*d*<sub>7</sub>/50% PBS in D<sub>2</sub>O (pH 7.4) with 5 molar equiv. of GSH, as observed at different time points (0 or 24 h) under air or inert (N<sub>2</sub>) atmospheres. Red sphere indicates one of two β-CH<sub>2</sub> resonances of [Ir<sub>2</sub>(η<sup>5</sup>-Cp\*)<sub>2</sub>(μ-SG)<sub>3</sub>]<sup>+</sup> and GSSG, and green sphere indicates the Cp\* resonance of the dinuclear [Ir<sub>2</sub>(η<sup>5</sup>-Cp\*)<sub>2</sub>(μ-SG)<sub>3</sub>]<sup>+</sup> species.

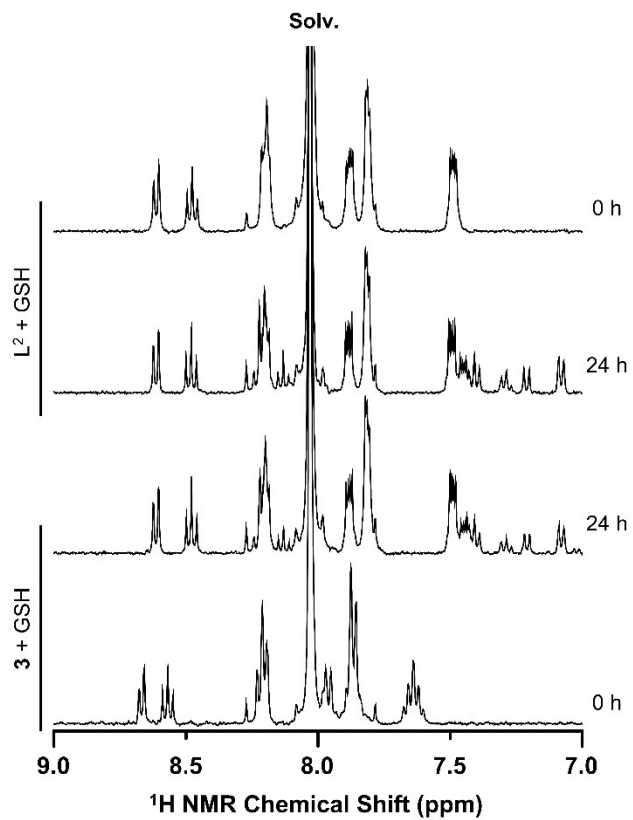


**Figure S28.** <sup>1</sup>H NMR studies of free ligand L<sup>2</sup> (given with **3** for comparative purposes) with 5 molar equivalents of GSH in 50% DMF-*d*<sub>7</sub>/50% PBS in D<sub>2</sub>O (pH 7.4), as observed at different time points (0 h or 24 h). Solv = DMF-*d*<sub>7</sub>.

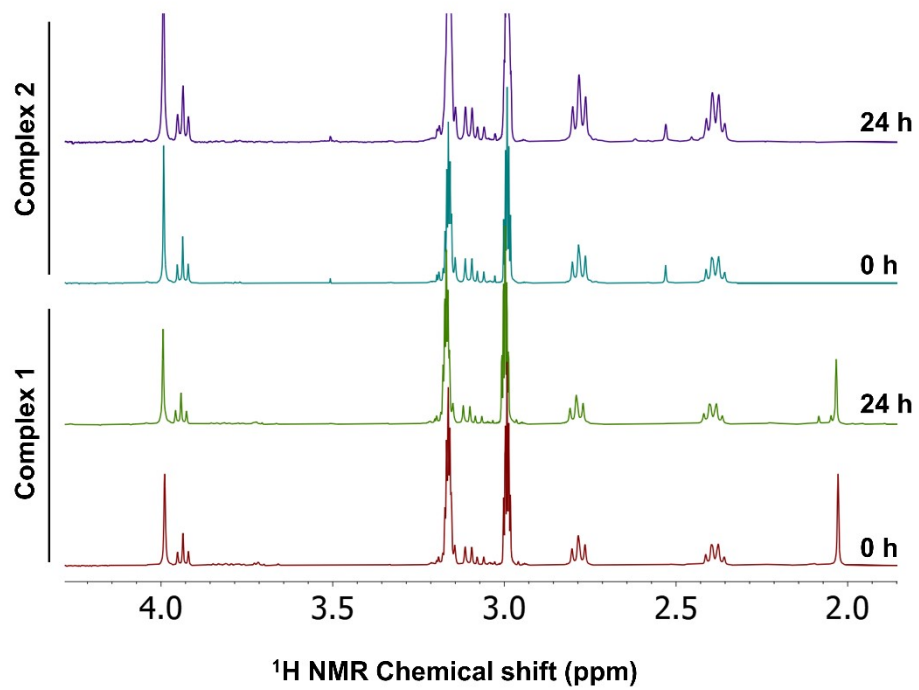


**Figure S29.** <sup>1</sup>H NMR studies of complexes **1** and **2** in 50% DMF-*d*<sub>7</sub>/50% PBS in D<sub>2</sub>O (pH 7.4) with 5 molar equiv. of GSH, as observed at different time points (0 h or 24 h).

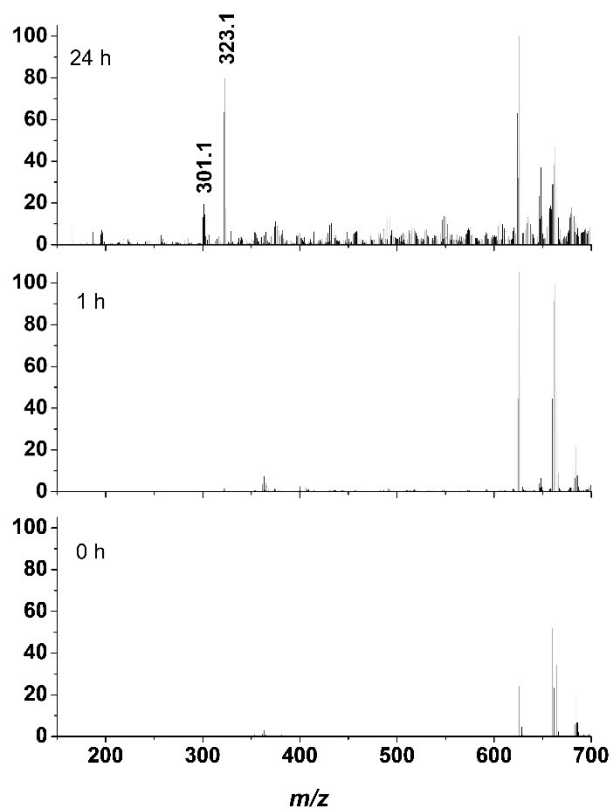


**Figure S30.** ESI+ mass spectra of complex **3** (dissolved in MeOH) mixed with 5 molar equiv. of reduced glutathione (GSH), as observed at different time points.  $m/z$  301.1 and 323.1 for  $L^2$  and ( $L^2+Na$ ), respectively, and their hydrazo-derivatives; ESI+ = positive electrospray ionization mode.

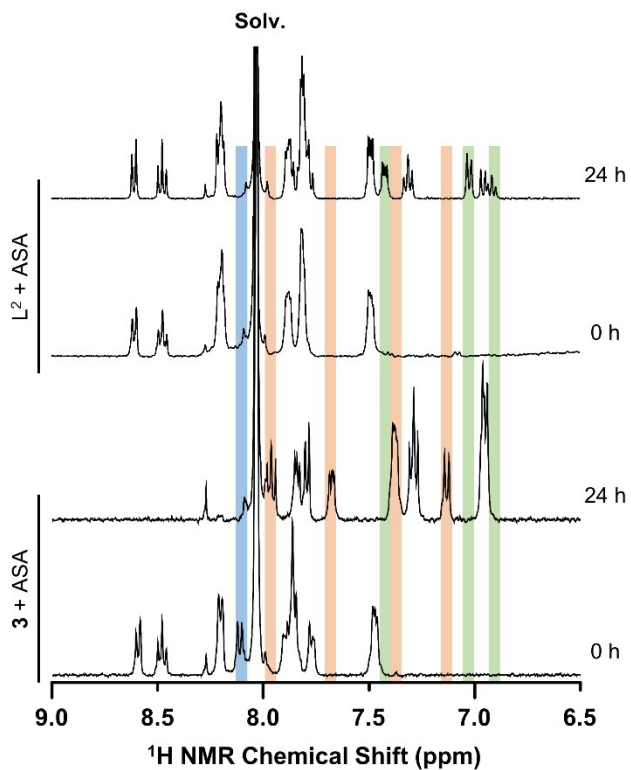


**Figure S31.** <sup>1</sup>H NMR studies of complex **3** (given with  $L^2$  for comparative purposes) with 5 molar equivalents of ascorbic acid in 50%  $DMF-d_7$ /50% PBS in  $D_2O$  (pH 7.4), as observed at different time points. Blue region - coordinated  $L^2$ ; red region - coordinated hydrazo form of  $L^2$ ; green region - free hydrazo form of  $L^2$ . Solv =  $DMF-d_7$ .

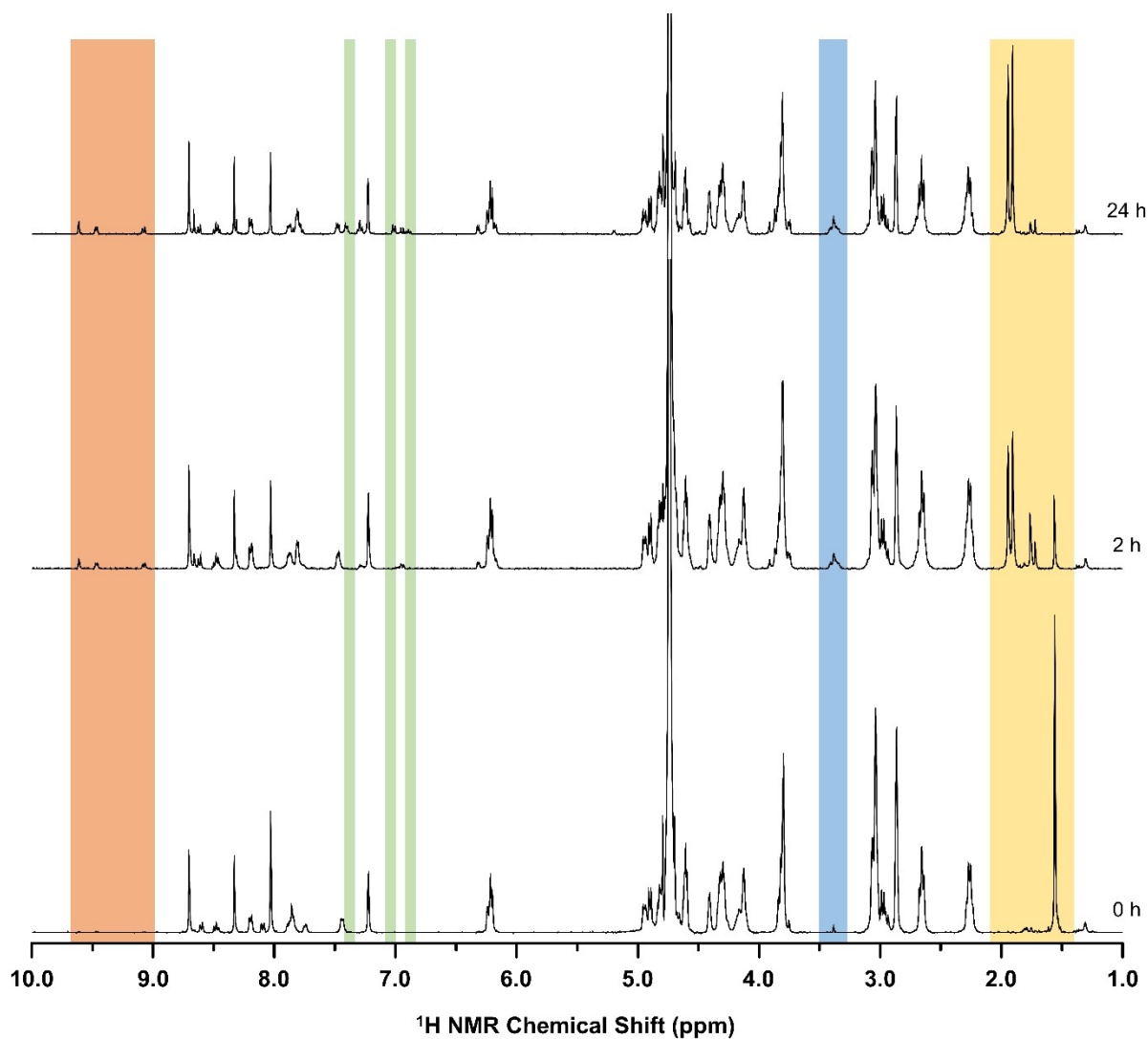


**Figure S32.** <sup>1</sup>H NMR studies of complex **3** in 50% DMF-*d*<sub>7</sub>/50% PBS in D<sub>2</sub>O (pH 7.4) with 5 molar equiv. of GSH and NADH, as observed at different time points. Red region - NAD<sup>+</sup>; green region - free hydrazo form of L<sup>2</sup>; blue region - one of two β-CH<sub>2</sub> resonances of [Ir<sub>2</sub>(η<sup>5</sup>-Cp\*)<sub>2</sub>(μ-SG)<sub>3</sub>]<sup>+</sup> (**Ir2**) and GSSG; yellow region - Cp\* signals.

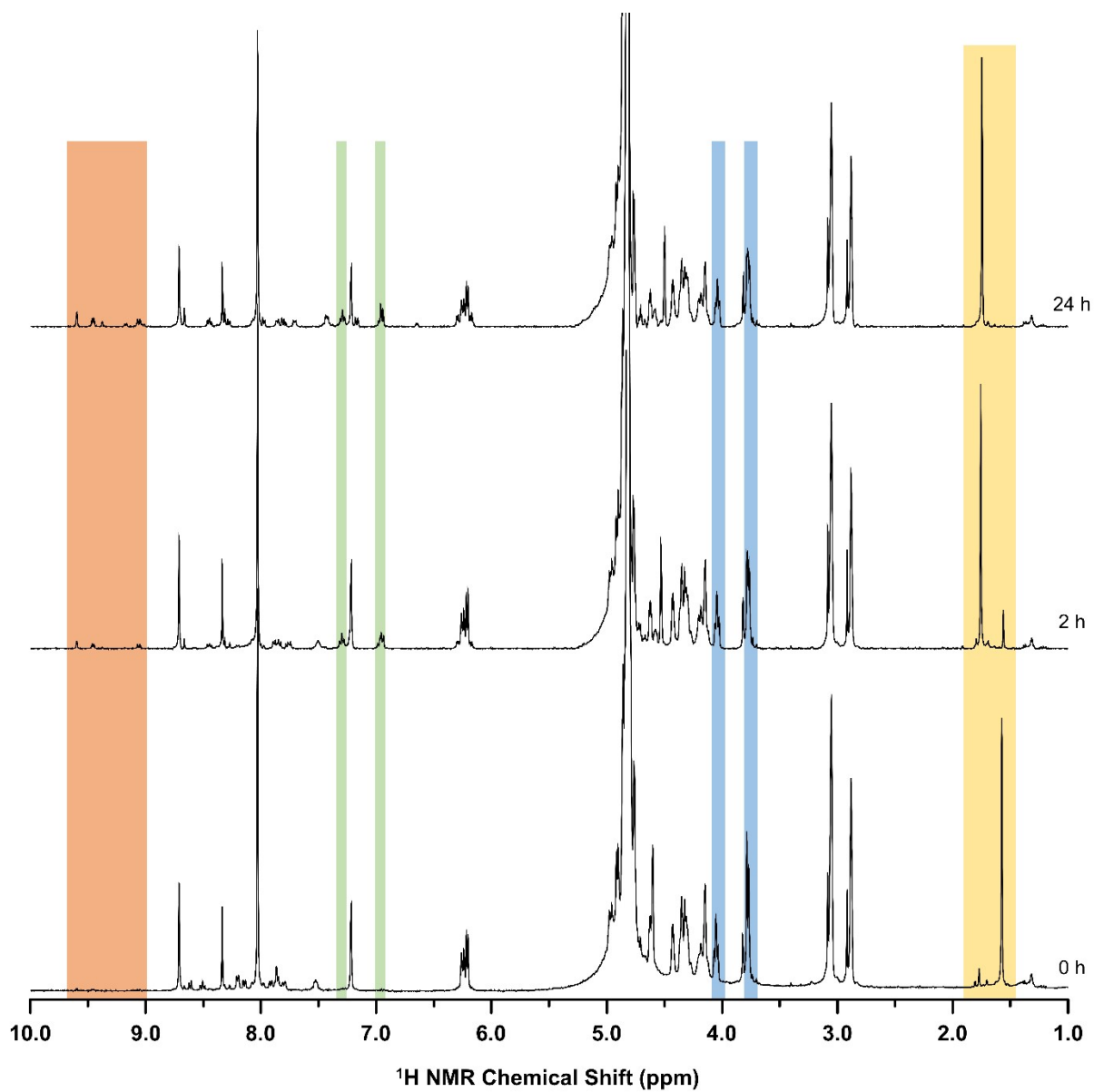


**Figure S33.** <sup>1</sup>H NMR studies of complex **3** in 50% DMF-*d*<sub>7</sub>/50% PBS in D<sub>2</sub>O (pH 7.4) with 5 molar equiv. of ASA and NADH, as observed at different time points. Red region - NAD<sup>+</sup>; green region - coordinated hydrazo form of L<sup>2</sup>; blue region - ASA; yellow region - Cp\* signals.

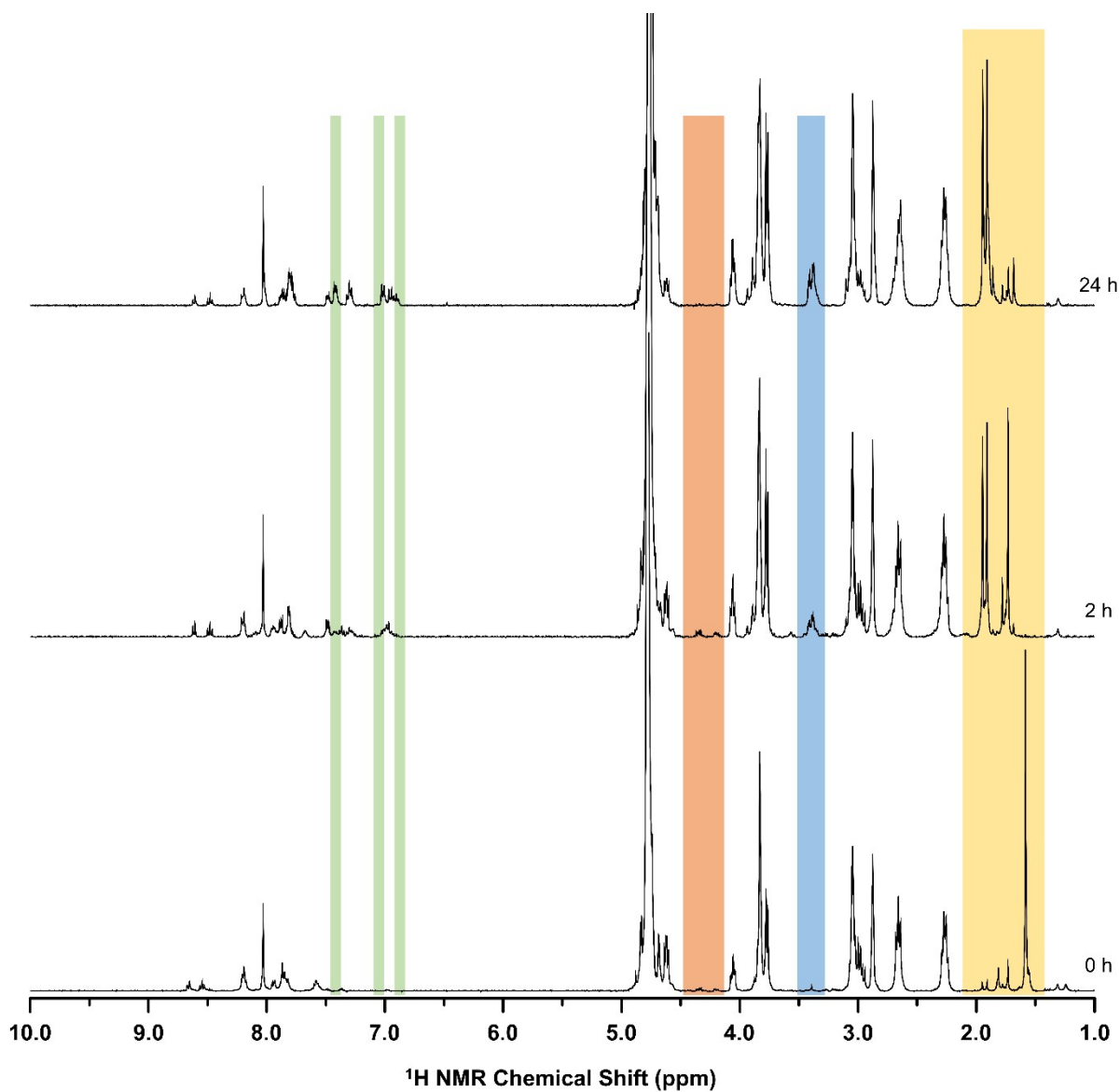


**Figure S34.** <sup>1</sup>H NMR studies of complex **3** in 50% DMF-*d*<sub>7</sub>/50% PBS in D<sub>2</sub>O (pH 7.4) with 5 molar equiv. of GSH and ASA, as observed at different time points. Green region - free hydrazo form of L<sup>2</sup>; red region - DHA; blue region - one of two β-CH<sub>2</sub> resonances of [Ir<sub>2</sub>(η<sup>5</sup>-Cp\*)<sub>2</sub>(μ-SG)<sub>3</sub>]<sup>+</sup> (**Ir2**) and GSSG; yellow region - Cp\* signals.

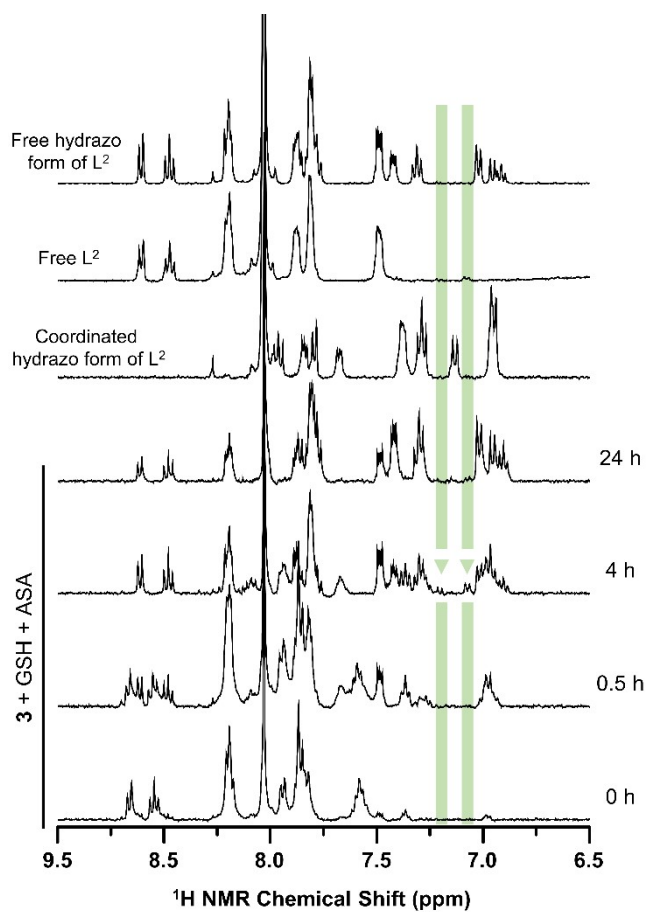


**Figure S35.** <sup>1</sup>H NMR studies of complex **3** in 50% DMF-*d*<sub>7</sub>/50% PBS in D<sub>2</sub>O (pH 7.4) with 5 molar equiv. of GSH and ASA, as observed at different time points. Green triangles - new signals assignable to the covalent adduct [Ir(η<sup>5</sup>-Cp\*)(L<sup>2</sup>)(SG)]<sup>+</sup>.

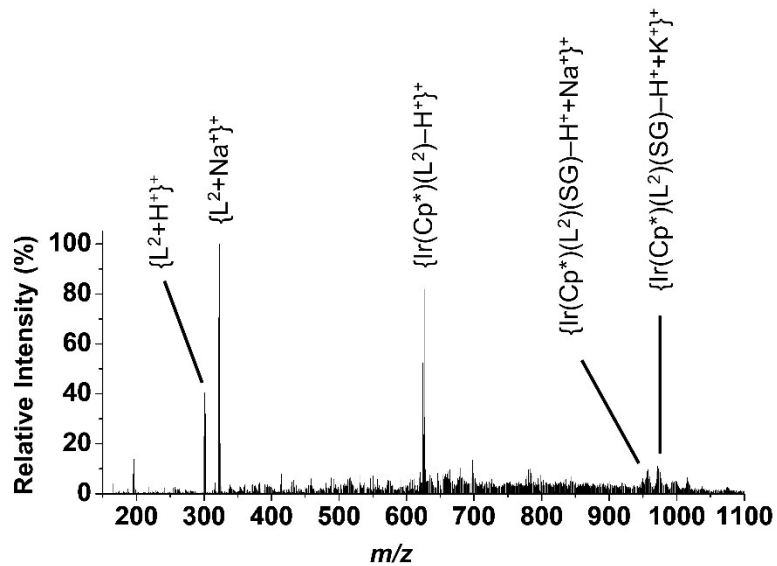


**Figure S36.** ESI+ mass spectra of complex **3** (dissolved in MeOH) mixed with 5 molar equiv. of reduced glutathione (GSH) and ascorbic acid (ASA), recorded after 4 h of standing at room temperature in the dark; ESI+ = positive electrospray ionization mode.

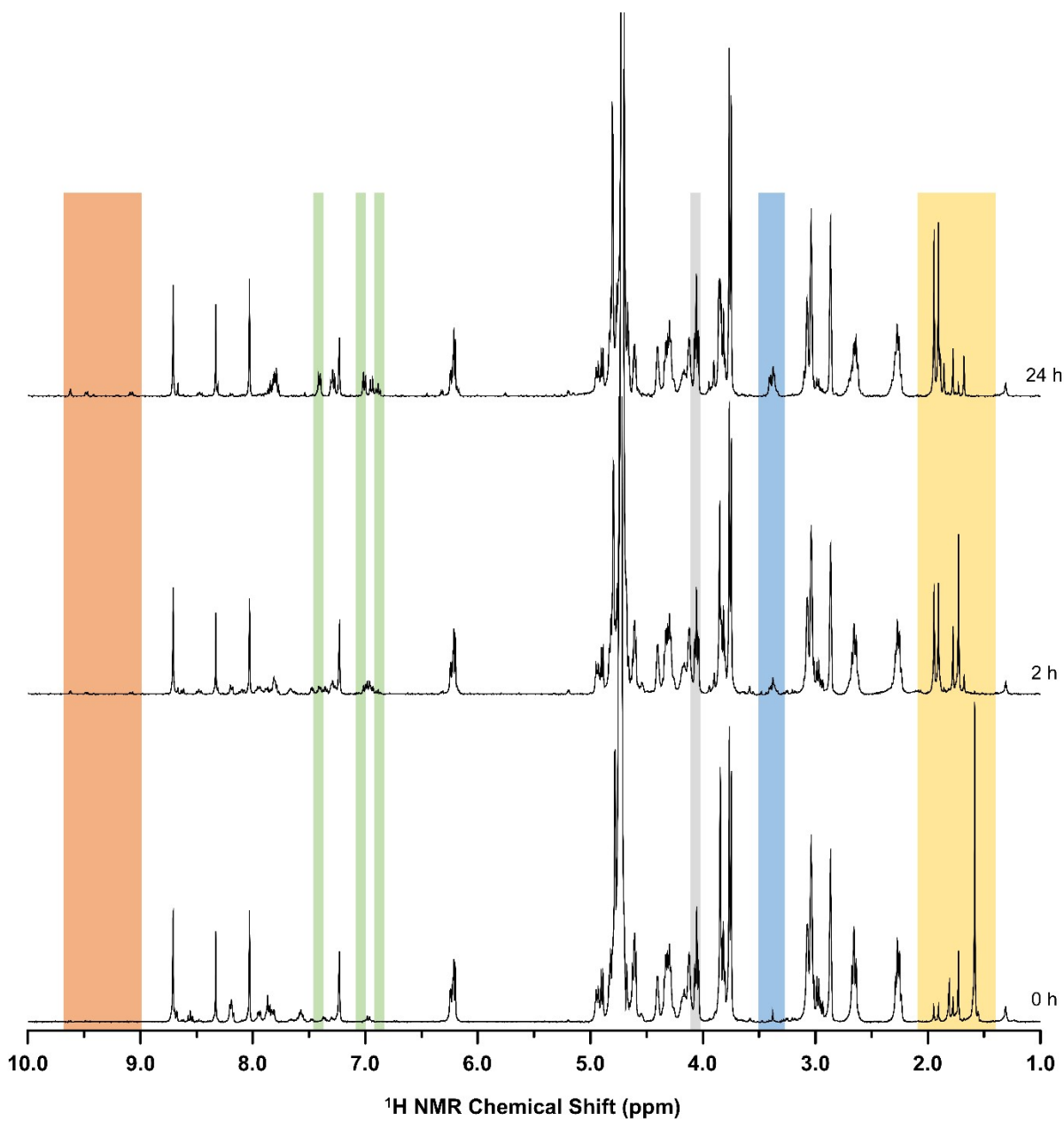


**Figure S37.** <sup>1</sup>H NMR studies of complex **3** in 50% DMF-*d*<sub>7</sub>/50% PBS in D<sub>2</sub>O (pH 7.4) with 5 molar equiv. of GSH, NADH and ASA, as observed at different time points. Red region - NAD<sup>+</sup>; green region - coordinated hydrazo form of L<sup>2</sup>; blue region - ASA; yellow region - Cp\* signals.

## References

1. M. A. Bennett, T.-N. Huang, T. W. Matheson and A. K. Smith, ( $\eta^6$ -Hexamethylbenzene)Ruthenium Complexes, *Inorg. Synth.*, 1982, **21**, 74–78.
2. C. White, A. Yates and P. M. Maitlis, ( $\eta^5$ -Pentamethylcyclopentadienyl)Rhodium and -Iridium Compounds, *Inorg. Synth.*, 1992, **29**, 228–234.
3. P. Štarha, Z. Trávníček, J. Vančo and Z. Dvořák, Half-Sandwich Ru(II) Halogenido, Valproato and 4-Phenylbutyrato Complexes Containing 2,2'-Dipyridylamine: Synthesis, Characterization, Solution Chemistry and In Vitro Cytotoxicity, *Molecules*, 2018, **21**, 1725.
4. P. Štarha, Z. Travnicek, H. Crlikova, J. Vančo, J. Kašpárková and Z. Dvořák, Half-Sandwich Ir(III) Complex of N1-Pyridyl-7-azaindole Exceeds Cytotoxicity of Cisplatin at Various Human Cancer Cells and 3D Multicellular Tumor Spheroids, *Organometallics*, 2018, **37**, 2749–2759.
5. J. Koziskova, F. Hahn, J. Richter and J. Kožíšek, Comparison of Different Absorption Corrections on the Model Structure of tetrakis( $\mu_2$ -acetato)-diaqua-di-copper(II), *Acta Chim. Slovaca*, 2016, **9**, 136–140.
6. M. L. Palatinus and G. Chapuis, Superflip - a Computer Program for the Solution of Crystal Structures by Charge Flipping in Arbitrary Dimensions, *J. Appl. Crystallogr.*, 2007, **40**, 786–790.
7. G. M. Sheldrick, *SHELXT* - Integrated Space-Group and Crystal-Structure Determination, *Acta Crystallogr. A*, 2015, **71**, 3–8.
8. L. J. Bourhis, O. V. Dolomanov, R. J. Gildea, J. A. K. Howard and H. Puschmann, The Anatomy of a Comprehensive Constrained, Restrained Refinement Program for the Modern Computing Environment - *Olex2* Dissected, *Acta Crystallogr. C*, 2015, **71**, 59–75.
9. G. M. Sheldrick, Crystal Structure Refinement with *SHELXL*, *Acta Crystallogr. C*, 2015, **71**, 3–8.
10. O. V. Dolomanov, L. J. Bourhis, R. J. Gildea, J. A. K. Howard and H. Puschmann, *OLEX2*: A Complete Structure Solution, Refinement and Analysis Program, *J. Appl. Crystallogr.*, 2009, **42**, 339–341.
11. J. Li, L. Guo, Z. Tian, S. Zhang, Z. Xu, Y. Han, R. Li, Y. Li and Z. Liu, Half-Sandwich Iridium and Ruthenium Complexes: Effective Tracking in Cells and Anticancer Studies, *Inorg. Chem.*, 2018, **57**, 13552–13563.
12. V. V. Pavlishchuk and A. W. Addison, Conversion constants for redox potentials measured versus different reference electrodes in acetonitrile solutions at 25 °C, *Inorg. Chim. Acta*, 2000, **298**, 97–102.
13. F. Neese, F. Wennmohs, U. Becker and C. Riplinger, The ORCA Quantum Chemistry Program Package, *J. Chem. Phys.*, 2020, **152**, 224108.
14. F. Neese, Software Update: the ORCA Program System, Version 4.0, *WIREs Comput. Mol. Sci.*, 2018, **8**, e1327.
15. C. Adamo and V. Barone, Toward Reliable Density Functional Methods without Adjustable Parameters: The PBE0 Model, *J. Chem. Phys.*, 1999, **110**, 6158–6170.
16. A. Najibi and L. Goerigk, DFT-D4 Counterparts of Leading Meta-Generalized-Gradient Approximation and Hybrid Density Functionals for Energetics and Geometries, *J. Comput. Chem.*, 2020, **41**, 2562–2572.
17. C. van Wüllen, Molecular Density Functional Calculations in the Regular Relativistic Approximation: Method, Application to Coinage Metal Diatomics, Hydrides, Fluorides and

- Chlorides, and Comparison with First-Order Relativistic Calculations, *J. Chem. Phys.*, 1998, **109**, 392–399.
18. J. D. Rolfes, F. Neese and D. A. Pantazis, All-Electron Scalar Relativistic Basis Sets for the Elements Rb–Xe, *J. Comput. Chem.*, 2020, **41**, 1842–1849.
  19. D. A. Pantazis, X.-Y. Chen, C. R. Landis and F. Neese, All-Electron Scalar Relativistic Basis Sets for Third-Row Transition Metal Atoms, *J. Chem. Theory Comput.*, 2008, **4**, 908–919.
  20. F. Weigend and R. Ahlrichs, Balanced Basis Sets of Split Valence, Triple Zeta Valence and Quadruple Zeta Valence Quality for H to Rn: Design and Assessment of Accuracy, *Phys. Chem. Chem. Phys.*, 2005, **7**, 3297–3305.
  21. F. Weigend, Accurate Coulomb-Fitting Basis Sets for H to Rn, *Phys. Chem. Chem. Phys.*, 2006, **8**, 1057–1065.
  22. F. Neese, F. Wennmohs, A. Hansen and U. Becker, Efficient, Approximate and Parallel Hartree–Fock and Hybrid DFT Calculations. A ‘Chain-of-Spheres’ Algorithm for the Hartree–Fock Exchange, *Chem. Phys.*, 2009, **356**, 98–109.
  23. R. Izsák and F. Neese, An Overlap Fitted Chain of Spheres Exchange Method, *J. Chem. Phys.*, 2011, **135**, 144105.
  24. V. Barone and M. Cossi, Quantum Calculation of Molecular Energies and Energy Gradients in Solution by a Conductor Solvent Model, *J. Phys. Chem. A*, 1998, **102**, 1995–2001.
  25. A. W. Lange and J. M. Herbert, A smooth, Nonsingular, and Faithful Discretization Scheme for Polarizable Continuum Models: The Switching/Gaussian Approach, *J. Chem. Phys.*, 2010, **133**, 244111.
  26. C. J. Cramer, *Essentials of Computational Chemistry: Theories and Models*, 2<sup>nd</sup> Edition, Wiley, 2004.
  27. V. Ásgeirsson, B. O. Birgisson, R. Bjornsson, U. Becker, F. Neese, C. Riplinger and H. Jónsson, Nudged Elastic Band Method for Molecular Reactions Using Energy-Weighted Springs Combined with Eigenvector Following, *J. Chem. Theory Comput.*, 2021, **17**, 4929–4945.